High Order Weighted Essentially Nonoscillatory Schemes for Convection Dominated Problems*

Chi-Wang Shu†

Abstract. High order accurate weighted essentially nonoscillatory (WENO) schemes are relatively new but have gained rapid popularity in numerical solutions of hyperbolic partial differential equations (PDEs) and other convection dominated problems. The main advantage of such schemes is their capability to achieve arbitrarily high order formal accuracy in smooth regions while maintaining stable, nonoscillatory, and sharp discontinuity transitions. The schemes are thus especially suitable for problems containing both strong discontinuities and complex smooth solution features. WENO schemes are robust and do not require the user to tune parameters. At the heart of the WENO schemes is actually an approximation procedure not directly related to PDEs, hence the WENO procedure can also be used in many non-PDE applications. In this paper we review the history and basic formulation of WENO schemes, outline the main ideas in using WENO schemes to solve various hyperbolic PDEs and other convection dominated problems, and present a collection of applications in areas including computational fluid dynamics, computational astronomy and astrophysics, semiconductor device simulation, traffic flow models, computational biology, and some non-PDE applications. Finally, we mention a few topics concerning WENO schemes that are currently under investigation.

Key words. weighted essentially nonoscillatory (WENO) scheme, hyperbolic partial differential equations, convection dominated problems, computational fluid dynamics, computational astronomy and astrophysics, semiconductor device simulation, traffic flow models, computational biology

AMS subject classification. 65M06

DOI. 10.1137/070679065

1. Introduction. In this paper we review a relatively recent yet quite popular class of high order numerical methods for solving convection dominated partial differential equations (PDEs), in particular hyperbolic conservation laws. This class of schemes is termed weighted essentially nonoscillatory (WENO) schemes. At the heart of the WENO schemes is actually an approximation procedure not directly related to PDEs, hence the WENO procedure can also be used in many non-PDE applications.

The first WENO scheme was introduced in 1994 by Liu, Osher, and Chan in their pioneering paper [106], in which a third order accurate finite volume WENO scheme was designed. In 1996, Jiang and Shu [78] provided a general framework to construct

arbitrary order accurate finite difference WENO schemes, which are more efficient for multidimensional calculations. Most applications use the fifth order accurate WENO scheme designed in [78].

For convection dominated problems, especially for hyperbolic conservation laws, the main challenge to the design of numerical schemes is the presence of discontinuities (such as shocks and contact discontinuities in high speed gas dynamics) or sharp transition layers. This happens often in complex solution structures also including smooth components such as vortices and acoustic waves. Traditional low order numerical methods, such as the first order Godunov scheme [52] or the Roe scheme [139], can resolve the discontinuities monotonically without spurious numerical oscillations; however, they often smear some of these discontinuities (for example, the contact discontinuities) excessively. They also contain relatively large numerical dissipation in the smooth part of the solution, hence many grid points are required to resolve complicated smooth structures such as vortices and acoustic waves, especially for long time simulation. The so-called high resolution schemes designed in the 1970s and 1980s, represented by MUSCL schemes [167], TVD schemes [63], and PPM schemes [34], are usually second order accurate in smooth regions and can resolve discontinuities monotonically with a sharper transition than first order schemes. These high resolution schemes are very popular in applications. They are often the best choice in terms of a balance between computational cost and desired resolution, especially for problems with solutions dominated by shocks or other discontinuities with relatively simple structures between these discontinuities. For problems containing both shocks and complicated *smooth* solution structure, such as shock interaction with vortices or acoustic waves, schemes with higher order of accuracy which can resolve shocks in an essentially nonoscillatory (ENO) fashion are desirable. A successful class of such high order schemes is the class of ENO schemes of Harten et al. [66, 153, 154]. ENO schemes can be designed for any order of accuracy, and they produce sharp and ENO shock transitions even for strong shocks. WENO schemes are constructed based on the successful ENO schemes with additional advantages, which explains their rapid widespread popularity in applications. Even though a high order WENO scheme may use 3 to 10 times more CPU time than a second order high resolution scheme, depending on the specific algorithm components and computer implementation, it may still be computationally advantageous for many application problems because of its high accuracy and resolution power. Many of the details regarding WENO schemes can be found in the lecture notes [149, 150].

The essential idea of the WENO schemes is an adaptive interpolation or reconstruction procedure. This is explained in detail in section 2. In section 3 we describe the finite difference and finite volume WENO schemes for solving hyperbolic conservation laws. We start with the simple one-dimensional scalar case and then remark on the procedures necessary to generalize the algorithm to handle systems, multispace dimensions including unstructured meshes, boundary conditions, and time discretization. In section 4 we describe finite difference WENO schemes for solving the Hamilton–Jacobi equations on structured and unstructured meshes. In section 5 we describe the relationship between the WENO schemes and a few other classes of high order schemes for convection dominated problems, including the discontinuous Galerkin methods, compact schemes, spectral methods, wavelets and multiresolution methods, and dispersion optimized finite difference schemes for wave propagation problems. Rather than surveying the details of these methods, we emphasize efforts in combining their advantages with the WENO procedure. Section 6 contains a collection of applications of WENO schemes in science and engineering, in diverse

areas including computational fluid dynamics, computational astronomy and astrophysics, semiconductor device simulation, traffic flow models, computational biology, and some non-PDE applications. Finally, in section 7 we mention a few topics concerning WENO schemes that are currently under investigation.

2. WENO Interpolation and Reconstruction. As mentioned before, at the heart of the WENO schemes is actually an approximation procedure not directly related to PDEs. In this section we will use simple examples to describe this approximation procedure.

2.1. WENO Interpolation. We first look at the problem of interpolation. Assume that we have a mesh $\cdots < x_1 < x_2 < x_3 < \cdots$. Further assume, for simplicity, that the mesh is uniform, i.e., $\Delta x = x_{i+1} - x_i$ is a constant. Therefore we may take $x_i = i\,\Delta x$. We assume that we are given the point values of a function $u(x)$ at the grid points in this mesh, that is, $u_i = u(x_i)$ is known for all i. We would like to find an approximation of the function $u(x)$ at a point other than the nodes x_i, for example, at the half nodes $x_{i+\frac{1}{2}}$.

This can be handled by the traditional approach of interpolation. For example, we could find a unique polynomial of degree at most two, denoted by $p_1(x)$, which interpolates the function $u(x)$ at the mesh points in the stencil $S_1 = \{x_{i-2}, x_{i-1}, x_i\}$. That is, we have $p_1(x_j) = u_j$ for $j = i-2,\, i-1,\, i$. We could then use $u_{i+\frac{1}{2}}^{(1)} \equiv p_1(x_{i+\frac{1}{2}})$ as an approximation to the value $u(x_{i+\frac{1}{2}})$. A simple algebra leads to the explicit formula for this approximation,

$$(2.1) \qquad u_{i+\frac{1}{2}}^{(1)} = \frac{3}{8}u_{i-2} - \frac{5}{4}u_{i-1} + \frac{15}{8}u_i.$$

From elementary numerical analysis, we know that this approximation is third order accurate,

$$u_{i+\frac{1}{2}}^{(1)} - u(x_{i+\frac{1}{2}}) = O(\Delta x^3),$$

if the function $u(x)$ is smooth in the stencil S_1. Similarly, if we chose a different stencil $S_2 = \{x_{i-1}, x_i, x_{i+1}\}$, we would obtain a different interpolation polynomial $p_2(x)$ satisfying $p_2(x_j) = u_j$ for $j = i-1,\, i,\, i+1$. We then obtain a different approximation $u_{i+\frac{1}{2}}^{(2)} \equiv p_2(x_{i+\frac{1}{2}})$ to $u(x_{i+\frac{1}{2}})$, given explicitly as

$$(2.2) \qquad u_{i+\frac{1}{2}}^{(2)} = -\frac{1}{8}u_{i-1} + \frac{3}{4}u_i + \frac{3}{8}u_{i+1},$$

which is also third order accurate,

$$u_{i+\frac{1}{2}}^{(2)} - u(x_{i+\frac{1}{2}}) = O(\Delta x^3),$$

provided that the function $u(x)$ is smooth in the stencil S_2. Finally, a third stencil $S_3 = \{x_i, x_{i+1}, x_{i+2}\}$ would lead to yet another interpolation polynomial $p_3(x)$ satisfying $p_3(x_j) = u_j$ for $j = i,\, i+1,\, i+2$ and giving another approximation $u_{i+\frac{1}{2}}^{(3)} \equiv p_3(x_{i+\frac{1}{2}})$, or

$$(2.3) \qquad u_{i+\frac{1}{2}}^{(3)} = \frac{3}{8}u_i + \frac{3}{4}u_{i+1} - \frac{1}{8}u_{i+2},$$

which is of course also third order accurate,

$$u^{(3)}_{i+\frac{1}{2}} - u(x_{i+\frac{1}{2}}) = O(\Delta x^3),$$

provided that the function $u(x)$ is smooth in the stencil S_3.

If the function $u(x)$ is globally smooth, all three approximations $u^{(1)}_{i+\frac{1}{2}}$, $u^{(2)}_{i+\frac{1}{2}}$, and $u^{(3)}_{i+\frac{1}{2}}$ obtained above are third order accurate. One could choose one of them based on other considerations, for example, to make the coefficient of the error term $O(\Delta x^3)$ as small as possible (which would then favor the approximation $u^{(2)}_{i+\frac{1}{2}}$ or $u^{(3)}_{i+\frac{1}{2}}$, whose stencils include the point $x_{i+\frac{1}{2}}$, over the approximation $u^{(1)}_{i+\frac{1}{2}}$). If using them to design finite difference approximations for solving time-dependent PDEs, the choice of these stencils would also need to be restricted by the linear stability of the resulting scheme.

If we used the large stencil $S = \{x_{i-2}, x_{i-1}, x_i, x_{i+1}, x_{i+2}\}$, which is the union of all three third order stencils S_1, S_2, and S_3, then we would be able to obtain an interpolation polynomial $p(x)$ of degree at most four, satisfying $p(x_j) = u_j$ for $j = i-2, i-1, i, i+1, i+2$ and giving an approximation $u_{i+\frac{1}{2}} \equiv p(x_{i+\frac{1}{2}})$, or

$$(2.4) \qquad u_{i+\frac{1}{2}} = \frac{3}{128}u_{i-2} - \frac{5}{32}u_{i-1} + \frac{45}{64}u_i + \frac{15}{32}u_{i+1} - \frac{5}{128}u_{i+2},$$

which is fifth order accurate,

$$u_{i+\frac{1}{2}} - u(x_{i+\frac{1}{2}}) = O(\Delta x^5),$$

provided that the function $u(x)$ is smooth in the large stencil S.

An important observation, which will be used later in our WENO interpolation, is that the fifth order approximation $u_{i+\frac{1}{2}}$, defined in (2.4) and based on the large stencil S, can be written as a linear convex combination of the three third order approximations $u^{(1)}_{i+\frac{1}{2}}$, $u^{(2)}_{i+\frac{1}{2}}$, and $u^{(3)}_{i+\frac{1}{2}}$, defined by (2.1), (2.2), (2.3) and based on the three small stencils S_1, S_2, and S_3, respectively:

$$(2.5) \qquad u_{i+\frac{1}{2}} = \gamma_1 u^{(1)}_{i+\frac{1}{2}} + \gamma_2 u^{(2)}_{i+\frac{1}{2}} + \gamma_3 u^{(3)}_{i+\frac{1}{2}},$$

where the constants γ_1, γ_2, and γ_3, satisfying $\gamma_1 + \gamma_2 + \gamma_3 = 1$, are usually referred to as the *linear weights* in the WENO literature. In this case they are given as

$$\gamma_1 = \frac{1}{16}, \qquad \gamma_2 = \frac{5}{8}, \qquad \gamma_3 = \frac{5}{16}.$$

Now we assume that $u(x)$ is only piecewise smooth and is discontinuous at isolated points. For such a function $u(x)$, if Δx is small enough that the large stencil S does not contain two discontinuity points of $u(x)$, then for each index i we have the following two possibilities:

1. The function $u(x)$ is smooth in the big stencil S. In this case, all three third order approximations $u^{(1)}_{i+\frac{1}{2}}$, $u^{(2)}_{i+\frac{1}{2}}$, and $u^{(3)}_{i+\frac{1}{2}}$ can be used, as well as the fifth order approximation $u_{i+\frac{1}{2}}$ given by (2.4) or by (2.5).

2. The function $u(x)$ has a discontinuity point in $[x_{i-2}, x_{i+2}]$. In this case there is at least one stencil out of S_1, S_2, and S_3 in which the function $u(x)$ is smooth. That is, at least one of the three third order approximations $u^{(1)}_{i+\frac{1}{2}}$, $u^{(2)}_{i+\frac{1}{2}}$, and $u^{(3)}_{i+\frac{1}{2}}$ is still a valid third order accurate approximation to $u(x_{i+\frac{1}{2}})$.

We remark that there may be situations in which *all* small stencils contain the discontinuity. For example, this would be the case if we considered only the two small stencils S_2 and S_3 and the function $u(x)$ had a discontinuity point in (x_i, x_{i+1}). For this interpolation problem, such situations can be avoided if we have a small stencil which does not include (x_i, x_{i+1}), for example, S_1. Unfortunately, for solving PDEs and because of the requirement of conservation, it is usually not possible to avoid such situations. It turns out that this seemingly difficult case is actually not problematic. This is because in such situations the interpolation polynomial $p(x)$, as well as $p_2(x)$ and $p_3(x)$, are all essentially monotone in the interval $[x_i, x_{i+1}]$. That is, in this interval which contains a discontinuity of $u(x)$, no spurious overshoot or undershoot would appear. To demonstrate this fact, let us assume for simplicity that $u_j = 1$ for $j \leq i$ and $u_j = 0$ for $j \geq i + 1$; that is, $u(x)$ is a step function with a discontinuity in (x_i, x_{i+1}). The polynomial $p(x)$ interpolates $u(x)$ in the stencil S; that is, $p(x_{i-2}) = p(x_{i-1}) = p(x_i) = 1$ and $p(x_{i+1}) = p(x_{i+2}) = 0$. Therefore, there is at least one zero of $p'(x)$ in each of the intervals (x_{i-2}, x_{i-1}), (x_{i-1}, x_i), and (x_{i+1}, x_{i+2}). However, $p'(x)$ is a polynomial of degree at most three, so it has at most three distinct zeros that are all accounted for in the three intervals above. We thus conclude that $p'(x)$ does *not* have a zero in the interval $[x_i, x_{i+1}]$, hence $p(x)$ is monotone in this interval. This result also holds when $u(x)$ is a more general piecewise smooth function [67]. Therefore, the interpolation to $u(x_{i+\frac{1}{2}})$ in this case will *not* be oscillatory, even though it may not be accurate.

The classical ENO way of treating the two cases above is to choose *one* of the three approximations $u_{i+\frac{1}{2}}^{(1)}$, $u_{i+\frac{1}{2}}^{(2)}$, and $u_{i+\frac{1}{2}}^{(3)}$, defined by (2.1), (2.2), (2.3) and based on the three stencils S_1, S_2, and S_3, respectively, using the fact of the local smoothness of the given data u_j for $i - 2 \leq j \leq i + 2$, measured by divided differences. This would guarantee third order accuracy and ENO performance since $u(x)$ is smooth in at least one of the three stencils S_1, S_2, and S_3.

On the other hand, the WENO idea is to choose the final approximation as a convex combination of the three third order approximations $u_{i+\frac{1}{2}}^{(1)}$, $u_{i+\frac{1}{2}}^{(2)}$, and $u_{i+\frac{1}{2}}^{(3)}$:

$$(2.6) \qquad u_{i+\frac{1}{2}} = w_1 u_{i+\frac{1}{2}}^{(1)} + w_2 u_{i+\frac{1}{2}}^{(2)} + w_3 u_{i+\frac{1}{2}}^{(3)},$$

where $w_j \geq 0$, $w_1 + w_2 + w_3 = 1$. Notice that, even for the difficult situation described above when all the small stencils contain the discontinuity, the WENO approximation $u_{i+\frac{1}{2}}$ would still be monotone, since it is a convex combination of monotone approximations. We would hope that the *nonlinear weights* w_j satisfy the following requirements:

- $w_j \approx \gamma_j$ if $u(x)$ is smooth in the big stencil S;
- $w_j \approx 0$ if $u(x)$ has a discontinuity in the stencil S_j but is smooth in at least one of the other two stencils.

It can be verified [78] that, as long as

$$(2.7) \qquad w_j = \gamma_j + O(\Delta x^2),$$

the WENO interpolation $u_{i+\frac{1}{2}}$ is fifth order accurate,

$$u_{i+\frac{1}{2}} - u(x_{i+\frac{1}{2}}) = O(\Delta x^5),$$

when the function $u(x)$ is smooth in the large stencil S, namely, in the first case above, just as in the original linear interpolation given by (2.4) or by (2.5). The

second requirement above would guarantee a nonoscillatory, at least third order accurate WENO approximation $u_{i+\frac{1}{2}}$ given by (2.6) in the second case above, since the contribution from any stencil containing the discontinuity of $u(x)$ has an essentially zero weight. In our choice of the WENO weights below, $w_j = O(\Delta x^4)$.

The choice of the nonlinear weights w_j relies on the *smoothness indicator* β_j, which measures the relative smoothness of the function $u(x)$ in the stencil S_j. The larger this smoothness indicator β_j, the less smooth the function $u(x)$ is in the stencil S_j. In most of the WENO papers, this smoothness indicator is chosen as in [78],

$$(2.8) \qquad \beta_j = \sum_{l=1}^{k} \Delta x^{2l-1} \int_{x_{i-\frac{1}{2}}}^{x_{i+\frac{1}{2}}} \left(\frac{d^l}{dx^l} p_j(x) \right)^2 dx,$$

where k is the polynomial degree of $p_j(x)$ (in our example, $k = 2$). This is clearly just a scaled sum of the square L^2 norms of all the derivatives of the relevant interpolation polynomial $p_j(x)$ in the relevant interval $[x_{i-\frac{1}{2}}, x_{i+\frac{1}{2}}]$, where the interpolating point is located. The scaling factor Δx^{2l-1} is to make sure that the final explicit formulas for the smoothness indicators do not depend on the mesh size Δx. In our example, we can easily express these explicit formulas as

$$\beta_1 = \frac{1}{3} \left(4u_{i-2}^2 - 19u_{i-2}u_{i-1} + 25u_{i-1}^2 + 11u_{i-2}u_i - 31u_{i-1}u_i + 10u_i^2 \right),$$

$$(2.9) \quad \beta_2 = \frac{1}{3} \left(4u_{i-1}^2 - 13u_{i-1}u_i + 13u_i^2 + 5u_{i-1}u_{i+1} - 13u_iu_{i+1} + 4u_{i+1}^2 \right),$$

$$\beta_3 = \frac{1}{3} \left(10u_i^2 - 31u_iu_{i+1} + 25u_{i+1}^2 + 11u_iu_{i+2} - 19u_{i+1}u_{i+2} + 4u_{i+2}^2 \right).$$

Notice that these smoothness indicators are quadratic functions of the values of $u(x)$ in the relevant stencils. Equipped with these smoothness indicators, we can now define the nonlinear weights as

$$(2.10) \qquad w_j = \frac{\tilde{w}_j}{\tilde{w}_1 + \tilde{w}_2 + \tilde{w}_3}, \qquad \text{with} \quad \tilde{w}_j = \frac{\gamma_j}{(\varepsilon + \beta_j)^2}.$$

Here ε is a small positive number used to avoid the denominator becoming zero and is typically chosen to be $\varepsilon = 10^{-6}$ in actual calculations. It can also be chosen to be a small number relative to the size of the typical u_i under calculation. We refer to [78, 70] for verification that such nonlinear weights do satisfy the accuracy condition (2.7) for the reconstruction case. Notice that the choice of the unnormalized nonlinear weight $\tilde{w}_j$ defined in (2.10) is inversely proportional to the square of the smoothness indicator β_j; hence it is smaller if β_j is larger, namely, if the function $u(x)$ in the stencil S_j is less smooth. Of course, one could also choose $\tilde{w}_j$ to be another decreasing function of β_j, such as a function inversely proportional to β_j^p for another $p \neq 2$ or a function proportional to $e^{-\alpha\beta_j}$ for some $\alpha > 0$. These different choices were tested and the choice in (2.10) was made in [78] after considering both cost and performance.

2.2. WENO Reconstruction. Compared to the problem of WENO interpolation described in the previous subsection, the problem of WENO reconstruction is more relevant to numerical solutions of conservation laws. To describe this reconstruction problem, we still use the uniform mesh $x_i = i\,\Delta x$ and the half points $x_{i+\frac{1}{2}} = \frac{1}{2}(x_i +$

x_{i+1}). Instead of assuming that the grid values u_i of the function $u(x)$ are known, we assume that its cell averages

$$\bar{u}_i = \frac{1}{\Delta x} \int_{x_{i-\frac{1}{2}}}^{x_{i+\frac{1}{2}}} u(x)dx$$

over the intervals $I_i = (x_{i-\frac{1}{2}}, x_{i+\frac{1}{2}})$ are given. We would again like to find an approximation of the function $u(x)$ at a given point, for example, at the half nodes $x_{i+\frac{1}{2}}$.

Even though this problem looks different from that of interpolation, they are in fact closely related. If we define the primitive function of $u(x)$ by

$$U(x) = \int_{x_{-\frac{1}{2}}}^{x} u(\xi)d\xi,$$

where the lower limit $x_{-\frac{1}{2}}$ is irrelevant and can be replaced by any fixed point, then we clearly have

$$U(x_{i+\frac{1}{2}}) = \int_{x_{-\frac{1}{2}}}^{x_{i+\frac{1}{2}}} u(\xi)d\xi = \sum_{l=0}^{i} \int_{x_{l-\frac{1}{2}}}^{x_{l+\frac{1}{2}}} u(\xi)d\xi = \sum_{l=0}^{i} \Delta x \, \bar{u}_l.$$

That is, knowing all the cell averages $\bar{u}_l$, we also know the point values of the primitive function $U(x_{i+\frac{1}{2}})$ at all half nodes. Therefore, interpolation polynomials can be constructed for the primitive function $U(x)$. The derivative of such an interpolation polynomial for $U(x)$ can then be used as an approximation to $u(x) = U'(x)$.

We carry out this procedure for an example similar to the one described in the previous subsection. Let $P_1(x)$ be the polynomial of degree at most three which interpolates the function $U(x)$ at the four points $x_{j+\frac{1}{2}}$, $j = i-3, i-2, i-1, i$, and let $p_1(x) = P_1'(x)$; then it is easy to verify that $p_1(x)$ is the unique polynomial of degree at most two which "reconstructs" the function $u(x)$ over the stencil $S_1 = \{I_{i-2}, I_{i-1}, I_i\}$, in the sense that

$$(\bar{p}_1)_j = \frac{1}{\Delta x} \int_{x_{j-\frac{1}{2}}}^{x_{j+\frac{1}{2}}} p_1(x)dx = \bar{u}_j, \qquad j = i-2, i-1, i.$$

One could then use $u_{i+\frac{1}{2}}^{(1)} \equiv p_1(x_{i+\frac{1}{2}})$ as an approximation to the value $u(x_{i+\frac{1}{2}})$. A simple algebra leads to the explicit formula for this approximation,

$$(2.11) \qquad u_{i+\frac{1}{2}}^{(1)} = \frac{1}{3}\bar{u}_{i-2} - \frac{7}{6}\bar{u}_{i-1} + \frac{11}{6}\bar{u}_i.$$

From the relationship $p_1(x) = P_1'(x)$ and the elementary numerical analysis about the interpolation polynomial $P_1(x)$, we know that this approximation is third order accurate,

$$u_{i+\frac{1}{2}}^{(1)} - u(x_{i+\frac{1}{2}}) = O(\Delta x^3),$$

if the function $u(x)$ is smooth in the stencil S_1. Similarly, a different stencil $S_2 = \{I_{i-1}, I_i, I_{i+1}\}$ would yield a different reconstruction polynomial $p_2(x)$ satisfying

$(\bar{p}_2)_j = \bar{u}_j$ for $j = i - 1$, i, $i + 1$, hence a different approximation $u^{(2)}_{i+\frac{1}{2}} \equiv p_2(x_{i+\frac{1}{2}})$ to $u(x_{i+\frac{1}{2}})$, given explicitly as

$$(2.12) \qquad u^{(2)}_{i+\frac{1}{2}} = -\frac{1}{6}\bar{u}_{i-1} + \frac{5}{6}\bar{u}_i + \frac{1}{3}\bar{u}_{i+1},$$

which is also third order accurate,

$$u^{(2)}_{i+\frac{1}{2}} - u(x_{i+\frac{1}{2}}) = O(\Delta x^3),$$

provided that the function $u(x)$ is smooth in the stencil S_2. Finally, a third stencil $S_3 = \{I_i, I_{i+1}, I_{i+2}\}$ would lead to a third reconstruction polynomial $p_3(x)$ satisfying $(\bar{p}_3)_j = \bar{u}_j$ for $j = i$, $i + 1$, $i + 2$ and giving another approximation $u^{(3)}_{i+\frac{1}{2}} \equiv p_3(x_{i+\frac{1}{2}})$, or

$$(2.13) \qquad u^{(3)}_{i+\frac{1}{2}} = \frac{1}{3}\bar{u}_i + \frac{5}{6}\bar{u}_{i+1} - \frac{1}{6}\bar{u}_{i+2},$$

which is of course also third order accurate,

$$u^{(3)}_{i+\frac{1}{2}} - u(x_{i+\frac{1}{2}}) = O(\Delta x^3),$$

provided that the function $u(x)$ is smooth in the stencil S_3.

If we used the large stencil $S = \{I_{i-2}, I_{i-1}, I_i, I_{i+1}, I_{i+2}\}$, which is the union of all three third order stencils S_1, S_2, and S_3, then we would be able to obtain a reconstruction polynomial $p(x)$ of degree at most four, satisfying $\bar{p}_j = \bar{u}_j$ for $j = i - 2$, $i - 1$, i, $i + 1$, $i + 2$ and giving an approximation $u_{i+\frac{1}{2}} \equiv p(x_{i+\frac{1}{2}})$, or

$$(2.14) \qquad u_{i+\frac{1}{2}} = \frac{1}{30}\bar{u}_{i-2} - \frac{13}{60}\bar{u}_{i-1} + \frac{47}{60}\bar{u}_i + \frac{9}{20}\bar{u}_{i+1} - \frac{1}{20}\bar{u}_{i+2},$$

which is fifth order accurate,

$$u_{i+\frac{1}{2}} - u(x_{i+\frac{1}{2}}) = O(\Delta x^5),$$

provided that the function $u(x)$ is smooth in the large stencil S.

As before, the fifth order approximation $u_{i+\frac{1}{2}}$, defined in (2.14) and based on the large stencil S, can be written as a linear convex combination of the three third order approximations $u^{(1)}_{i+\frac{1}{2}}$, $u^{(2)}_{i+\frac{1}{2}}$, and $u^{(3)}_{i+\frac{1}{2}}$, defined by (2.11), (2.12), (2.13) and based on the three small stencils S_1, S_2, and S_3, respectively:

$$(2.15) \qquad u_{i+\frac{1}{2}} = \gamma_1 u^{(1)}_{i+\frac{1}{2}} + \gamma_2 u^{(2)}_{i+\frac{1}{2}} + \gamma_3 u^{(3)}_{i+\frac{1}{2}},$$

where the linear weights γ_1, γ_2, and γ_3, satisfying $\gamma_1 + \gamma_2 + \gamma_3 = 1$, are given in this reconstruction case as

$$\gamma_1 = \frac{1}{10}, \qquad \gamma_2 = \frac{3}{5}, \qquad \gamma_3 = \frac{3}{10}.$$

In the WENO literature, the reconstruction (2.15) is sometimes referred to as a *linear reconstruction*, not because it is a reconstruction using a linear function, but because the weights γ_1, γ_2, and γ_3 are constant linear weights. The WENO idea is again

to choose the final approximation as a convex combination of the three third order approximations,

$$(2.16) \qquad u_{i+\frac{1}{2}} = w_1 u_{i+\frac{1}{2}}^{(1)} + w_2 u_{i+\frac{1}{2}}^{(2)} + w_3 u_{i+\frac{1}{2}}^{(3)},$$

where the nonlinear weights $w_j \geq 0$ are determined again by (2.10), with the smoothness indicators determined by (2.8). However, since the reconstruction polynomials $p_j(x)$ are different from the interpolation polynomials there, the explicit formulas of the smoothness indicators would change from (2.9) to

$$(2.17) \qquad \begin{aligned} \beta_1 &= \frac{13}{12} \left(\bar{u}_{i-2} - 2\bar{u}_{i-1} + \bar{u}_i \right)^2 + \frac{1}{4} \left(\bar{u}_{i-2} - 4\bar{u}_{i-1} + 3\bar{u}_i \right)^2, \\ \beta_2 &= \frac{13}{12} \left(\bar{u}_{i-1} - 2\bar{u}_i + \bar{u}_{i+1} \right)^2 + \frac{1}{4} \left(\bar{u}_{i-1} - \bar{u}_{i+1} \right)^2, \\ \beta_3 &= \frac{13}{12} \left(\bar{u}_i - 2\bar{u}_{i+1} + \bar{u}_{i+2} \right)^2 + \frac{1}{4} \left(3\bar{u}_i - 4\bar{u}_{i+1} + \bar{u}_{i+2} \right)^2. \end{aligned}$$

2.3. Further Remarks. In this section we make several additional remarks about the WENO interpolation and reconstruction procedures.

2.3.1. History and Properties of WENO Interpolation and Reconstruction. The WENO interpolation problem discussed in section 2.1 was used in [142] to transfer information from one domain to another in a high order, nonoscillatory fashion for a multidomain WENO scheme. It was also used in [14] to build a high order Lagrangian-type method for solving Hamilton–Jacobi equations. In fact, in [14] it is proven that the interpolation polynomial $p(x)$ of degree at most $2k-1$ over the large stencil and the interpolation polynomials $p_l(x)$ of degree at most k over the k smaller substencils, whose union is the large stencil, are related by

$$p(x) = \sum_{l=1}^{k} \gamma_l(x) p_l(x),$$

where the linear weights $\gamma_l(x)$ are polynomials of degree at most $k-1$ and $\gamma_l(x) \geq 0$ for x in the common interval of all the substencils. By choosing x to be a specific point, e.g., $x = x_{i+\frac{1}{2}}$, we would recover results in section 2.1.

The WENO reconstruction problem discussed in section 2.2 is the building block of all WENO schemes for solving hyperbolic conservation laws. The third order version was discussed in the first WENO paper [106]. The fifth order version and the general framework for the smoothness indicator (2.8) were discussed in [78]. Higher order versions of this WENO reconstruction were discussed in [6].

2.3.2. Nonuniform and Multidimensional Meshes. Notice that neither the interpolation problem in section 2.1 nor the reconstruction problem in section 2.2 requires uniform or smooth meshes. We have used uniform meshes just for simplicity. In applications, e.g., [14, 146], WENO interpolations and reconstructions on nonuniform and nonsmooth meshes are used. The procedures are identical to those described in sections 2.1 and 2.2. The only difference is that the coefficients in, e.g., (2.1)–(2.4), the linear weights in, e.g., (2.5), and the coefficients in the explicit formulas of the smoothness indicators in, e.g., (2.9) would all become local constants depending on the mesh sizes in the stencil.

Two- and three-dimensional interpolation and reconstruction in Cartesian meshes can be performed in a dimension by dimension fashion, with the one-dimensional procedure discussed in the previous subsections used in each dimension. The interpolation

and reconstruction procedures can also be generalized to truly multidimensional unstructured meshes, for example, triangular meshes in two dimensions and tetrahedral meshes in three dimensions. However, the details of such generalization are much more involved than the one-dimensional version. We refer to, e.g., [10, 194] for the two-dimensional WENO interpolation and [73, 195] for the two- and three-dimensional WENO reconstructions on unstructured meshes.

2.3.3. Negative Linear Weights. In some of the WENO interpolation and reconstruction problems, especially in some of the latter, one might encounter linear weights γ_j in, e.g., (2.5) which are negative. Notice that these linear weights are determined uniquely by the accuracy requirement, hence if they happen to be negative, one must find a way to deal with the difficulty that the linear combination in, e.g., (2.5) is no longer a convex combination. If the usual WENO procedure is used without modification, oscillations and instability may appear. This is because a sum of monotone approximations with negative linear weights may become nonmonotone, even though the linear weights sum to one. A procedure to systematically modify the WENO procedure so that it is still stable and nonoscillatory in the presence of negative weights was developed in [146] and has been used in many later works, such as in [131], where this technique is used to construct high order central WENO schemes, in [127], where it is used to construct high order staggered finite difference WENO schemes, in [18], where it is used to construct high order WENO schemes for solving nonconservative hyperbolic systems, and in [117, 173, 174], where it is used to construct well-balanced high order WENO schemes for a class of balance laws including the shallow water equations.

Another approach to avoid the appearance of negative linear weights is to lower the accuracy requirement for the linear combination in, e.g., (2.5). For example, if we do not insist that $u_{i+\frac{1}{2}}$ in (2.5) achieves the maximum fifth order accuracy, but require it to be only fourth order accurate, then we have a free parameter in the determination of the linear weights γ_j. We can then explore this freedom to make all the linear weights positive. In the extreme case, we could require $u_{i+\frac{1}{2}}$ in (2.5) to be only third order accurate, so it is no more accurate than the approximation in each substencil. In this case *any* linear weights satisfying $\sum_j \gamma_j = 1$ would be fine. One could then, for example, take all the γ_j to be equal and positive, or choose the γ_j corresponding to the most symmetric substencil to be the largest. The drawback of this approach is of course a loss of accuracy: with the same large stencil, WENO schemes designed using this approach have a lower order accuracy than the "authentic" WENO schemes described in previous subsections. In [92], this technique is used to construct high order central WENO schemes, and in [50, 44, 45] it is used to construct finite volume WENO schemes on unstructured meshes.

2.3.4. Other WENO Procedures. Besides the interpolation and reconstruction problems discussed in sections 2.1 and 2.2, there are also many other problems in which a similar WENO procedure can be designed. Two such examples are as follows:

1. *Approximation to the derivative of a given function $u(x)$, given its point values $u_i = u(x_i)$.* The procedure is similar to the interpolation problem in section 2.1: one first finds interpolation polynomials $P_j(x)$ in the substencils and $P(x)$ in the large stencil, and then can find the linear weights γ_j so that

$$P'(x_i) = \sum_j \gamma_j P_j'(x_i)$$

if the approximation of the derivative at $x = x_i$ is needed. The remaining pro-

cedure is similar to those in section 2.1, except that the smoothness indicator (2.8) should be replaced by

$$\beta_j = \sum_{l=2}^{k} \Delta x^{2l-1} \int_{x_{i-\frac{1}{2}}}^{x_{i+\frac{1}{2}}} \left(\frac{d^l}{dx^l} P_j(x) \right)^2 dx.$$

This is because $P_j'(x)$ are our building blocks, hence the measurement of their smoothness should start from the second derivative of $P_j(x)$. This WENO derivative procedure is used in the design of WENO schemes for the Hamilton–Jacobi equations [77]. It is in fact also indirectly used in the WENO reconstruction procedure described in section 2.2 on the primitive function $U(x)$.

Clearly, one could also design similar WENO procedures to approximate the second or higher order derivatives of $u(x)$.

2. *Approximation to the integral of a given function $u(x)$, given its point values* $u_i = u(x_i)$. The procedure is parallel to the interpolation procedure described in section 2.1. For example, we could use the integral $I_i^{(1)} = \int_{x_{i-\frac{1}{2}}}^{x_{i+\frac{1}{2}}} p_1(x)dx$ of the unique polynomial $p_1(x)$ of degree at most two, which interpolates the function $u(x)$ at the mesh points in the stencil $S_1 = \{x_{i-2}, x_{i-1}, x_i\}$, to approximate the integral $\int_{x_{i-\frac{1}{2}}}^{x_{i+\frac{1}{2}}} u(x)dx$. A simple algebra leads to the explicit formula for this approximation,

$$(2.18) \qquad I_i^{(1)} = \Delta x \left(\frac{1}{24} u_{i-2} - \frac{1}{12} u_{i-1} + \frac{25}{24} u_i \right).$$

From elementary numerical analysis, we know that this approximation is fourth order accurate,

$$I_i^{(1)} - \int_{x_{i-\frac{1}{2}}}^{x_{i+\frac{1}{2}}} u(x)dx = O(\Delta x^4),$$

if the function $u(x)$ is smooth in the stencil S_1. Similarly, one obtains the approximations $I_i^{(2)}$ and $I_i^{(3)}$ based on the interpolation polynomials $p_2(x)$ and $p_3(x)$ over the stencils $S_2 = \{x_{i-1}, x_i, x_{i+1}\}$ and $S_3 = \{x_i, x_{i+1}, x_{i+2}\}$, respectively, given explicitly as

$$(2.19) \qquad I_i^{(2)} = \Delta x \left(\frac{1}{24} u_{i-1} + \frac{11}{12} u_i + \frac{1}{24} u_{i+1} \right)$$

and

$$(2.20) \qquad I_i^{(3)} = \Delta x \left(\frac{25}{24} u_i - \frac{1}{12} u_{i+1} + \frac{1}{24} u_{i+2} \right).$$

$I_i^{(2)}$ or $I_i^{(3)}$ is a fourth order accurate approximation to $\int_{x_{i-\frac{1}{2}}}^{x_{i+\frac{1}{2}}} u(x)dx$ if the function $u(x)$ is smooth in the relevant stencil S_2 or S_3, respectively. Finally, the approximation I_i based on the interpolating polynomial $p(x)$ over the large stencil $S = \{x_{i-2}, x_{i-1}, x_i, x_{i+1}, x_{i+2}\}$, given explicitly as
(2.21)

$$I_i = \Delta x \left(-\frac{17}{5760} u_{i-2} + \frac{77}{1440} u_{i-1} + \frac{863}{960} u_i + \frac{77}{1440} u_{i+1} - \frac{17}{5760} u_{i+2} \right),$$

is a sixth order approximation to $\int_{x_{i-\frac{1}{2}}}^{x_{i+\frac{1}{2}}} u(x)dx$ if the function $u(x)$ is smooth in the large stencil S. As before, this sixth order approximation I_i can be written as a linear combination of the three fourth order approximations $I_i^{(1)}$, $I_i^{(2)}$, and $I_i^{(3)}$:

$$(2.22) \qquad I_i = \gamma_1 I_i^{(1)} + \gamma_2 I_i^{(2)} + \gamma_3 I_i^{(3)},$$

where the linear weights γ_1, γ_2, and γ_3 are given in this case as

$$\gamma_1 = -\frac{17}{240}, \qquad \gamma_2 = \frac{137}{120}, \qquad \gamma_3 = -\frac{17}{240}.$$

Notice that this time some of the linear weights are negative. The remaining WENO procedure is similar to those in section 2.1, except that we would need to use the technique in [146] to handle the negative linear weights. The smoothness indicators are again given by (2.8) or explicitly by (2.9).

This WENO integration procedure is used in the design of high order residual distribution conservative finite difference WENO schemes in [25, 26].

2.3.5. Variations in the Choice of Smoothness Indicators and Nonlinear Weights. Finally, we mention that the choice of the nonlinear weights (2.10) is not unique. For example, [70] discusses another choice of the nonlinear weights, based on the same smoothness indicators (2.8), to enhance accuracy in smooth regions, especially at smooth extrema. The choice of the smoothness indicators (2.8) is also not unique. For example, [189] discusses another choice of the smoothness indicators to obtain better convergence to steady states of the WENO schemes for one- and two-dimensional nonlinear hyperbolic systems.

3. WENO Schemes for Hyperbolic Conservation Laws. Historically the main application of the WENO procedure has been to hyperbolic conservation laws, which in the one-dimensional scalar case have the form

$$(3.1) \qquad u_t + f(u)_x = 0.$$

More generally, a d-dimensional hyperbolic conservation law system is given by

$$(3.2) \qquad u_t + \sum_{j=1}^{d} f_j(u)_{x_j} = 0,$$

where u is a vector and any linear combination of the Jacobians $\sum_{j=1}^{d} \xi_j f_j'(u)$ for real ξ_j must have only real eigenvalues and a complete set of independent eigenvectors. We will mostly use the simple one-dimensional scalar equation (3.1) to describe the ideas of various WENO schemes. We will mention the generalizations to multidimensional problems in section 3.4 and to systems in section 3.5.

3.1. Finite Volume Schemes. A finite volume scheme approximates the conservation law (3.1) in its integral form

$$(3.3) \qquad \frac{d}{dt}\bar{u}_i + \frac{1}{\Delta x_i}\left(f(u_{i+\frac{1}{2}}) - f(u_{i-\frac{1}{2}}) \right) = 0,$$

where $\bar{u}_i = \frac{1}{\Delta x}\int_{x_{i-\frac{1}{2}}}^{x_{i+\frac{1}{2}}} u(x,t)dx$ is the spatial cell average of the solution $u(x,t)$ in the cell $I_i = (x_{i-\frac{1}{2}}, x_{i+\frac{1}{2}})$ as defined in section 2.2.

To convert (3.3) to a finite volume scheme, we take our computational variables as the cell averages $\{\bar{u}_i\}$ and use the WENO reconstruction procedure described in section 2.2 to obtain an approximation to $u_{i+\frac{1}{2}}$. An additional complication is that the solution to the conservation law (3.1) follows characteristics, hence a stable numerical scheme should also propagate its information in the same characteristic direction, which is referred to as *upwinding*. This is achieved by replacing $f(u_{i+\frac{1}{2}})$ by

$$\hat{f}\left(u_{i+\frac{1}{2}}^-, u_{i+\frac{1}{2}}^+\right),$$

where $\hat{f}(u^-, u^+)$ is a monotone numerical flux satisfying the following:
- $\hat{f}(u^-, u^+)$ is nondecreasing in its first argument u^- and nonincreasing in its second argument u^+, symbolically $\hat{f}(\uparrow, \downarrow)$;
- $\hat{f}(u^-, u^+)$ is consistent with the physical flux $f(u)$, i.e., $\hat{f}(u, u) = f(u)$;
- $\hat{f}(u^-, u^+)$ is Lipschitz continuous with respect to both arguments u^- and u^+.

Examples of monotone fluxes include
- the Godunov flux

$$\hat{f}^{God}(u^-, u^+) = \begin{cases} \min_{u^- \leq u \leq u^+} f(u) & \text{if } u^- \leq u^+, \\ \max_{u^+ \leq u \leq u^-} f(u) & \text{if } u^- > u^+; \end{cases}$$

- the Lax–Friedrichs flux

$$\hat{f}^{LF}(u^-, u^+) = \frac{1}{2}\left(f(u^-) + f(u^+) - \alpha(u^+ - u^-)\right),$$

where $\alpha = \max_u |f'(u)|$;
- the Engquist–Osher flux

$$\hat{f}^{LF}(u^-, u^+) = f^+(u^-) + f^-(u^+),$$

where

$$f^+(u) = f(0) + \int_0^u \max(f'(v), 0)dv, \qquad f^-(u) = \int_0^u \min(f'(v), 0)dv,$$

etc. We refer to, e.g., [90] and the references therein for a detailed discussion of monotone fluxes.

The approximations $u_{i+\frac{1}{2}}^-$ and $u_{i+\frac{1}{2}}^+$ are the WENO reconstructions from stencils one point biased to the left and one point biased to the right, respectively. For example, for a fifth order WENO scheme, the reconstruction $u_{i+\frac{1}{2}}^-$ uses the five-cell stencil

$$I_{i-2}, \ I_{i-1}, \ I_i, \ I_{i+1}, \ I_{i+2}$$

and the reconstruction $u_{i+\frac{1}{2}}^+$ uses the five-cell stencil

$$I_{i-1}, \ I_i, \ I_{i+1}, \ I_{i+2}, \ I_{i+3}.$$

The details of these WENO reconstructions were given in section 2.2.

The finite volume scheme described above can be written as a method-of-lines ordinary differential equation (ODE) system

$$(3.4) \qquad \frac{d}{dt}\bar{u}_i = -\frac{1}{\Delta x}\left[\hat{f}\left(u^-_{i+\frac{1}{2}}, u^+_{i+\frac{1}{2}}\right) - \hat{f}\left(u^-_{i-\frac{1}{2}}, u^+_{i-\frac{1}{2}}\right)\right] \equiv L(\bar{u})_i.$$

This ODE system can be discretized in time by the total variation diminishing (TVD) Runge–Kutta time discretization methods [153], also known as the strong stability preserving (SSP) methods [58]. A good property of such time discretization techniques is that they maintain stability in the total variation seminorm, or any other norm or seminorm, of the first order Euler forward method with the same spatial discretization. The most popular TVD Runge–Kutta time discretization method is the third order accurate version in [153]:

$$(3.5) \qquad \begin{aligned} \bar{u}^{(1)} &= \bar{u}^n + \Delta t L(\bar{u}^n), \\ \bar{u}^{(2)} &= \frac{3}{4}\bar{u}^n + \frac{1}{4}\bar{u}^{(1)} + \frac{1}{4}\Delta t L(\bar{u}^{(1)}), \\ \bar{u}^{n+1} &= \frac{1}{3}\bar{u}^n + \frac{2}{3}\bar{u}^{(2)} + \frac{2}{3}\Delta t L(\bar{u}^{(2)}). \end{aligned}$$

Such time discretizations are also used for the finite difference schemes discussed below. Multistep methods having this stability property are also available [148]. An alternative method of time discretization is via the Lax–Wendroff procedure, which performs a Taylor expansion in time and converts all time derivatives to spatial derivatives by repeatedly using the PDE, and finally discretizes all the spatial derivatives to the correct order of accuracy. See, e.g., [165, 132]. We remark that the fifth order WENO spatial discretization coupled with first order Euler forward time discretization or the second order Runge–Kutta method is linearly unstable [178], hence they should not be used even if the problem is steady state and no time accuracy is needed. For some applications, e.g., those with significantly varying mesh sizes, an implicit time discretization might be advantageous. We refer to, e.g., [51, 57] for discussions of implicit time discretization for WENO schemes.

3.2. Finite Difference Schemes. A finite difference scheme approximates the conservation law (3.1) directly. The computational variables are the point values $\{u_i\}$ of the solution, and the scheme is required to be in conservation form

$$(3.6) \qquad \frac{d}{dt}u_i + \frac{1}{\Delta x}\left(\hat{f}_{i+\frac{1}{2}} - \hat{f}_{i-\frac{1}{2}}\right) = 0,$$

where the numerical flux

$$(3.7) \qquad \hat{f}_{i+\frac{1}{2}} = \hat{f}\left(u_{i-p}, \ldots, u_{i+q}\right)$$

is consistent with the physical flux $\hat{f}(u, \ldots, u) = f(u)$ and is Lipschitz continuous with respect to all its arguments.

The scheme is rth order accurate if

$$\frac{1}{\Delta x}\left(\hat{f}_{i+\frac{1}{2}} - \hat{f}_{i-\frac{1}{2}}\right) = f(u)_x|_{x=x_i} + O(\Delta x^r),$$

when u is smooth in the stencil.

It seems that finite difference schemes are conceptually very different from finite volume schemes. However, the following simple lemma by Shu and Osher [154] establishes the relationship between the finite volume and finite difference schemes.

LEMMA 3.1. *If $h(x) = h_{\Delta x}(x)$ is implicitly defined as*

$$(3.8) \qquad \frac{1}{\Delta x} \int_{x-\frac{\Delta x}{2}}^{x+\frac{\Delta x}{2}} h(\xi)d\xi = f(u(x)),$$

then

$$\frac{1}{\Delta x} \left(h(x_{i+\frac{1}{2}}) - h(x_{i-\frac{1}{2}}) \right) = f(u)_x|_{x=x_i}.$$

The proof is straightforward: just take an x derivative on both sides of (3.8).

This simple lemma indicates that we can take the numerical flux in the finite difference scheme as

$$(3.9) \qquad \hat{f}_{i+\frac{1}{2}} = h(x_{i+\frac{1}{2}})$$

to ensure rth order accuracy, if the function $h(x)$ in the lemma can be computed to rth order accuracy.

In fact, the (implicit) definition (3.8) of $h(x)$ implies that

$$\bar{h}_i \equiv \frac{1}{\Delta x} \int_{x_{i-\frac{1}{2}}}^{x_{i+\frac{1}{2}}} h(\xi)d\xi = f(u_i)$$

is known for a finite difference scheme, since the point values u_i are the computational variables. Therefore, we are given the cell averages $\bar{h}_i$ of the function $h(x)$ and we would need to approximate its point values $h(x_{i+\frac{1}{2}})$ to high order accuracy to obtain the numerical flux $\hat{f}_{i+\frac{1}{2}}$ in (3.9). Hence, we can use the same WENO reconstruction procedure discussed in section 2.2 that has been used for finite volume schemes! This implies that a finite difference WENO code for the scalar one-dimensional conservation law (3.1) shares the main reconstruction subroutine with a finite volume WENO code. The only difference is the input-output pair: for a finite volume scheme, the input is the set of cell averages $\{\bar{u}_i\}$ and the output is the reconstructed values of the solution at the cell interfaces $\{u_{i+\frac{1}{2}}\}$; for a finite difference scheme, the input is the set of the point values of the physical flux $\{f(u_i)\}$ and the output is the numerical fluxes at the cell interfaces $\{\hat{f}_{i+\frac{1}{2}}\}$.

For the purpose of stability, the finite difference procedure described above is applied to $f^+(u)$ and $f^-(u)$ separately, where $f^\pm(u)$ correspond to a flux splitting

$$(3.10) \qquad f(u) = f^+(u) + f^-(u),$$

with

$$(3.11) \qquad \frac{d}{du}f^+(u) \geq 0, \qquad \frac{d}{du}f^-(u) \leq 0.$$

The reconstruction for $f^+(u)$ uses a biased stencil with one more point to the left, and that for $f^-(u)$ uses a biased stencil with one more point to the right, to ensure correct upwinding. We further require that $f^\pm(u)$ are as smooth functions of u as $f(u)$. The most commonly used flux splitting is the Lax–Friedrichs splitting

$$f^\pm(u) = \frac{1}{2} \left(f(u) \pm \alpha u \right),$$

with

$$\alpha = \max_u |f'(u)|.$$

However, other splittings can also be used. See, e.g., [78]. Notice that for any flux splitting (3.10) satisfying (3.11), $\hat{f}(u^-, u^+) = f^+(u^-) + f^-(u^+)$ is a monotone flux.

Finally, we remark that the finite difference WENO scheme discussed in this section can only be used on uniform or smooth meshes. Superficially, this is because Lemma 3.1 does not hold if Δx is not a constant. A deeper reason is given in [112]. A conservative finite difference scheme (3.6) with a local flux (3.7) cannot achieve higher than second order accuracy on arbitrary nonuniform nonsmooth meshes.

3.3. Comparison of Finite Volume and Finite Difference Schemes. We can now summarize the main features of the finite volume and the finite difference WENO schemes for solving the scalar one-dimensional conservation law (3.1) as follows.

- A finite volume WENO scheme
    1. is based on the cell averages $\{\bar{u}_i\}$ and uses the integral form (3.3) of the PDE;
    2. needs a WENO reconstruction described in section 2.2 with the cell averages $\{\bar{u}_i\}$ as input and with the reconstructed point values $\{u_{i+1/2}^\pm\}$ as output;
    3. can use any monotone flux $\hat{f}(u^-, u^+)$;
    4. can be applied to any meshes and does not need uniformity or smoothness of the meshes.
- A finite difference WENO scheme
    1. is based on the point values $\{u_i\}$ and uses the original PDE form (3.1) directly;
    2. needs a WENO reconstruction described in section 2.2 with the point values of the split fluxes $\{f^\pm(u_i)\}$ as input and with the numerical fluxes $\{\hat{f}_{i+\frac{1}{2}}^\pm\}$ as output;
    3. can only use monotone fluxes which correspond to smooth flux splitting $f(u) = f^+(u) + f^-(u)$ satisfying (3.11);
    4. can only be applied to uniform or smooth meshes.

Based on this comparison, we conclude that, for solving the one-dimensional scalar conservation law (3.1), the cost of the finite volume and the finite difference WENO schemes is the same (in fact they both involve the same WENO reconstruction procedure, the only difference being the input-output pair). The finite volume scheme is more flexible in its applicability to any monotone fluxes and to any nonuniform nonsmooth meshes. It would seem that the finite volume scheme is clearly the winner. This conclusion is valid for all one-dimensional calculations, including the case of one-dimensional systems. However, as we will see in the next subsection, the picture changes dramatically for multidimensional problems.

3.4. Multidimensional Problems. We use a two-dimensional scalar conservation law

$$(3.12) \qquad\qquad u_t + f(u)_x + g(u)_y = 0$$

to demonstrate finite volume and finite difference WENO schemes for multidimensional problems. Furthermore, we assume that we have a Cartesian mesh that is uniform in both x and y. If we integrate the PDE (3.12) over a typical cell $I_{ij} \equiv$

$[x_{i-\frac{1}{2}}, x_{i+\frac{1}{2}}] \times [y_{j-\frac{1}{2}}, y_{j+\frac{1}{2}}]$, we obtain the integral form

$$(3.13) \qquad \frac{d\tilde{\tilde{u}}_{ij}(t)}{dt} = -\frac{1}{\Delta x \Delta y} \left(\int_{y_{j-\frac{1}{2}}}^{y_{j+\frac{1}{2}}} f(u(x_{i+\frac{1}{2}}, y, t)) dy - \int_{y_{j-\frac{1}{2}}}^{y_{j+\frac{1}{2}}} f(u(x_{i-\frac{1}{2}}, y, t)) dy \right.$$
$$\left. + \int_{x_{i-\frac{1}{2}}}^{x_{i+\frac{1}{2}}} g(u(x, y_{j+\frac{1}{2}}, t)) dx - \int_{x_{i-\frac{1}{2}}}^{x_{i+\frac{1}{2}}} g(u(x, y_{j-\frac{1}{2}}, t)) dx \right),$$

where $\tilde{\tilde{u}}$ is the cell average

$$\tilde{\tilde{u}}_{ij}(t) \equiv \frac{1}{\Delta x \Delta y} \int_{y_{j-\frac{1}{2}}}^{y_{j+\frac{1}{2}}} \int_{x_{i-\frac{1}{2}}}^{x_{i+\frac{1}{2}}} u(x, y, t) dx dy.$$

In our notation, $\bar{v}$ stands for the cell average in x,

$$\bar{v}_{ij} = \frac{1}{\Delta x} \int_{x_{i-\frac{1}{2}}}^{x_{i+\frac{1}{2}}} v(x, y_j) dx,$$

and $\tilde{v}$ stands for the cell average in y,

$$\tilde{v}_{ij} = \frac{1}{\Delta y} \int_{y_{j-\frac{1}{2}}}^{y_{j+\frac{1}{2}}} v(x_i, y) dy.$$

We approximate the integral form (3.13) by a finite volume scheme

$$\frac{d\tilde{\tilde{u}}_{ij}(t)}{dt} = -\frac{1}{\Delta x}(\hat{f}_{i+\frac{1}{2},j} - \hat{f}_{i-\frac{1}{2},j}) - \frac{1}{\Delta y}(\hat{g}_{i,j+\frac{1}{2}} - \hat{g}_{i,j-\frac{1}{2}}),$$

where the numerical fluxes are given by

$$\hat{f}_{i+\frac{1}{2},j} \approx \frac{1}{\Delta y} \int_{y_{j-\frac{1}{2}}}^{y_{j+\frac{1}{2}}} f(u(x_{i+\frac{1}{2}}, y, t)) dy \equiv \tilde{f}_{i+\frac{1}{2},j},$$
$$\hat{g}_{i,j+\frac{1}{2}} \approx \frac{1}{\Delta x} \int_{x_{i-\frac{1}{2}}}^{x_{i+\frac{1}{2}}} g(u(x, y_{j+\frac{1}{2}}, t)) dx \equiv \bar{g}_{i,j+\frac{1}{2}}.$$

First, we look at the simple, linear constant coefficient case

$$u_t + au_x + bu_y = 0$$

for which we would have

$$\hat{f}_{i+\frac{1}{2},j} = a\tilde{u}_{i+\frac{1}{2},j}, \qquad \hat{g}_{i,j+\frac{1}{2}} = b\bar{u}_{i,j+\frac{1}{2}}.$$

In this case, we would need to perform only two one-dimensional WENO reconstructions

$$\{\tilde{\tilde{u}}_{ij}\} \rightarrow \{\tilde{u}_{i+\frac{1}{2},j}\} \qquad \text{for fixed } j$$

and

$$\{\tilde{\tilde{u}}_{ij}\} \rightarrow \{\bar{u}_{i,j+\frac{1}{2}}\} \qquad \text{for fixed } i,$$

and the cost is the same as in the one-dimensional case per cell per direction.

However, if the PDE (3.12) is nonlinear, namely, if $f(u)$ and $g(u)$ are nonlinear functions of u, then $f(\tilde{u}) \neq \widetilde{f(u)}$, hence we would need to perform two one-dimensional WENO reconstructions and one numerical integration (typically via Gauss quadratures of sufficient accuracy, which bears about the same cost as a reconstruction) to obtain the numerical flux $\hat{f}_{i+\frac{1}{2},j}$. Thus we would need to do

$$\{\tilde{\tilde{u}}_{ij}\} \ \rightarrow \ \{\tilde{u}_{i+\frac{1}{2},j}\} \ \rightarrow \ \{u_{i+\frac{1}{2},j+j_\alpha}\}_{\alpha=1}^{\alpha_g} \ \rightarrow \ \{\hat{f}_{i+\frac{1}{2},j}\},$$

where $\{j+j_\alpha\}_{\alpha=1}^{\alpha_g}$ are the Gaussian quadrature points for the interval $[y_{j-\frac{1}{2}}, y_{j+\frac{1}{2}}]$ with sufficiently high order of accuracy, and likewise for $\hat{g}_{i,j+\frac{1}{2}}$. This now has about three times the cost of the one-dimensional case per cell per direction. The situation will be much worse for three dimensions.

On the other hand, a finite difference scheme approximates the PDE form (3.12) directly and can proceed dimension by dimension. The scheme is

$$\frac{du_{ij}(t)}{dt} = -\frac{1}{\Delta x}(\hat{f}_{i+\frac{1}{2},j} - \hat{f}_{i-\frac{1}{2},j}) - \frac{1}{\Delta y}(\hat{g}_{i,j+\frac{1}{2}} - \hat{g}_{i,j-\frac{1}{2}}),$$

where the numerical flux $\hat{f}_{i+\frac{1}{2},j}$ can be computed from $\{u_{ij}\}$ with fixed j in exactly the same way as in the one-dimensional case described in section 3.2, and likewise for $\hat{g}_{i,j+\frac{1}{2}}$. Therefore, the computational cost is exactly the same as in the one-dimensional case per point per direction.

We can now conclude that in two dimensions, a finite volume scheme (of order of accuracy higher than two) is two to five times as expensive as a finite difference scheme of the same order of accuracy using the same mesh and the same reconstruction procedure, depending on the specific coding and type of computer. This discrepancy in cost is even bigger for three dimensions. We refer to [19] for a detailed comparison of multidimensional finite volume and finite difference schemes in the context of ENO reconstructions. Notice that this difference between finite volume and finite difference schemes is meaningful only for schemes of at least third order accuracy. For first and second order schemes there is no need to distinguish between a finite volume scheme and a finite difference scheme, since the cell average agrees with the value of the function at the cell centroid to second order accuracy.

We should also mention again that finite volume schemes are more flexible than finite difference schemes in terms of monotone fluxes and meshes. Conservative finite volume schemes can be designed on arbitrary meshes. This is a more significant advantage in multidimensions as one can design finite volume schemes on unstructured triangulations. However, because of the significant cost advantage, conservative finite difference WENO schemes are preferable whenever the problem allows a uniform Cartesian or a smooth curvilinear mesh.

3.5. Further Remarks. In this section we make several additional remarks about the WENO schemes.

3.5.1. Self-similarity. It should be remarked that the WENO reconstruction procedure, when the small parameter ε in (2.10) is chosen to be a small percentage of the typical size of u_i under calculation, is scale invariant. That is, the reconstruction does not change when the solution is amplified by a constant or when the mesh size Δx changes. The WENO finite volume and finite difference schemes are self-similar. That is, the numerical solution does not change if both the spatial mesh size Δx and the temporal mesh size Δt change by the same factor and $\lambda = \frac{\Delta t}{\Delta x}$ does not change.

Since the schemes are self-similar, we do not rely on explicit, mesh size Δx-dependent thresholds to determine whether there are discontinuities in the solution and their location. The numerical procedure automatically captures and handles discontinuities or sharp gradient regions when they appear, so that accuracy and stability are maintained. It is very important to have the numerical schemes satisfying these scale invariant and self-similar properties for many applications.

3.5.2. Convergence and Order of Accuracy. Since WENO schemes have smooth numerical fluxes and are dissipative, they can be shown to converge with high order accuracy using Strang's framework [158] when the solution of the PDE is smooth [78]. When the solution of the PDE becomes discontinuous, there is no general proof of stability and convergence for high order WENO schemes solving conservation laws. However, in applications WENO schemes perform well in terms of stability and resolution. As to numerically observed order of accuracy in smooth regions of a discontinuous solution, for scalar problems the full designed order of accuracy of the WENO scheme is achieved if we measure the error away from the discontinuity. For systems, because characteristics belonging to fields other than that of the discontinuity may cross the discontinuity and carry the numerical error at the discontinuity into smooth regions, pointwise errors in smooth regions of a high order WENO scheme may fail to achieve the designed order of accuracy, unless a subcell resolution technique [64] is used in the cells which contain shocks. We demonstrate this phenomenon by a nozzle flow simulation using a fourth order residual distribution WENO scheme in [25]. In Figure 3.1, we observe good resolution of the WENO numerical solution in comparison with the exact solution of the nonlinear Euler system with source terms. In Table 3.1, we observe that the designed fourth order accuracy is achieved both upstream and downstream of the shock if a subcell integration technique is applied in the cell which contains the shock, while the accuracy downstream of the shock has lower than the designed fourth order accuracy if no special treatment is performed in the cell which contains the shock. Nevertheless, even if the order of accuracy for the pointwise errors downstream of the shock may degenerate for a higher order WENO scheme, the magnitude of the errors is typically still much smaller than that of a lower order scheme on the same mesh. In practice, this is the advantage that we rely on when we use high order WENO schemes to solve complicated nonlinear systems with both shocks and smooth structures in the solutions.

Even though the pointwise errors for a high order scheme solving discontinuous solutions of a hyperbolic system may show a low order of accuracy, it is well known [87, 109] that the designed high order accuracy is maintained in integrated quantities of the numerical solution, such as moments against smooth functions, if the scheme and the PDE are both linear. With this information, we can postprocess the numerical solution to obtain the designed order of accuracy also for point values [54]. This is a strong theoretical justification for the use of high order schemes even for discontinuous solutions. Recently, [56] has given numerical evidence to indicate that such high order information may also be available for high order WENO schemes in solving *nonlinear* systems.

3.5.3. Systems and Source Terms. For systems of conservation laws, the WENO schemes have the same structure as those for the scalar cases discussed in the previous subsections. A monotone flux is replaced by an exact or approximate Riemann solver; see, e.g., [166]. The WENO reconstruction can be performed either componentwise or in local characteristic directions. Usually, componentwise reconstruction produces satisfactory results for schemes up to third order accuracy, while characteristic recon-
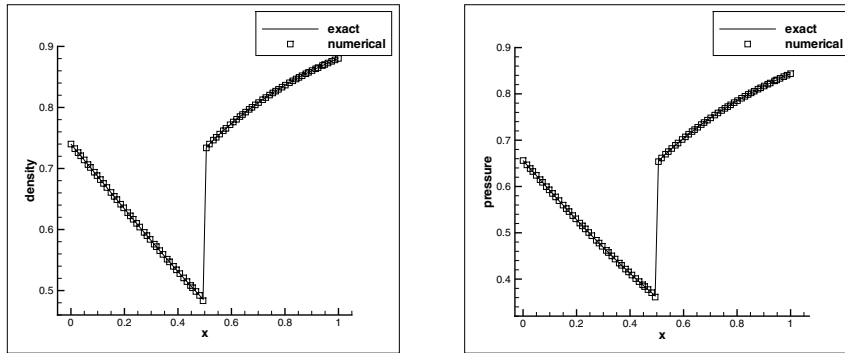
Fig. 3.1 *Reproduced from* [25]. *Fourth order residual distribution WENO scheme for the nozzle flow problem. Nonsmooth mesh with* 81 *cells. Solid lines: exact solution. Symbols: numerical solution. Left: density. Right: pressure.*

Table 3.1 *Reproduced from* [25]. *Fourth order residual distribution WENO scheme for the nozzle flow problem. Errors outside three cells around the shock and numerical orders of accuracy for the density ρ on nonsmooth meshes with N cells.*

	Subcell separate integrations in the cell which contains the shock							
	Before shock				After shock			
N	L^1 error	order	L^∞ error	order	L^1 error	order	L^∞ error	order
21	1.36E-07	-	7.09E-07	-	7.58E-06	-	3.35E-05	-
41	1.44E-08	3.23	6.13E-08	3.53	5.08E-07	3.90	2.19E-06	3.93
81	1.28E-09	3.49	4.85E-09	3.66	1.67E-08	4.93	6.61E-08	5.05
161	8.34E-11	3.94	3.11E-10	3.96	7.72E-10	4.43	3.00E-09	4.46
321	5.41E-12	3.95	2.00E-11	3.96	3.65E-11	4.40	1.36E-10	4.46
641	2.22E-13	4.60	1.20E-12	4.05	1.75E-12	4.38	4.92E-12	4.80
	Regular integration in the cell which contains the shock							
	Before shock				After shock			
N	L^1 error	order	L^∞ error	order	L^1 error	order	L^∞ error	order
21	1.36E-07	-	7.09E-07	-	1.75E-05	-	6.42E-05	-
41	1.44E-08	3.24	6.13E-08	3.53	4.38E-06	1.99	1.42E-05	2.18
81	1.28E-09	3.49	4.85E-09	3.66	1.11E-06	1.98	3.37E-06	2.07
161	8.34E-11	3.94	3.11E-10	3.96	2.34E-07	2.25	7.29E-07	2.21
321	5.41E-12	3.95	2.00E-11	3.96	5.81E-08	2.01	1.77E-07	2.04
641	2.22E-13	4.61	1.22E-12	4.04	8.15E-09	2.83	2.52E-08	2.81

struction produces better nonoscillatory results for higher order accuracy, albeit with an increased computational cost. Details about the local characteristic decomposition procedure can be found in many papers, e.g., [66, 153, 155].

When designing numerical schemes to solve hyperbolic systems with source terms,

$$(3.14) \qquad u_t + f(u)_x = g(u, x),$$

which are also called balance laws, it is a challenge for the scheme to maintain specific equilibria, that is, steady state solutions satisfying

$$f(u)_x = g(u, x)$$

exactly. This is because such equilibria are usually not constant or polynomial functions, so the truncation error of most schemes will not be exactly zero for such equilibria. A scheme which can maintain such equilibria is referred to as a *well-balanced*

scheme. The main advantage of well-balanced schemes, especially when they are also high order accurate for nonequilibrium solutions of (3.14), is that they can be used to resolve small perturbations of such equilibria, such as the small amplitude water waves from still water, very accurately without an excessively refined mesh. High order finite difference and finite volume WENO schemes which are well balanced for the still water solution of the shallow water equations, and a more general class of balance laws, were designed in [117, 168, 171, 172, 173, 174]. High order well-balanced finite difference WENO schemes for solving the hyperbolic models for chemosensitive movement were designed in [48]. High order finite volume WENO schemes that are well balanced for the moving steady water of the shallow water equations, which are much more difficult to construct, were designed in [118]. As an example, in Figure 3.2 we plot the water surface from a small perturbation (the perturbation amplitude is 1% of the still water height) for a later time, simulated by a fifth order well-balanced WENO scheme [171]. We can see clearly that the detailed structure of the evolution of such a small perturbation is resolved well even with the relatively coarse mesh of 200×100 points. If a regular, non-well-balanced WENO scheme is used, much smaller mesh sizes are needed to resolve the evolution of such small perturbations.

3.5.4. Power WENO Scheme and Boundary Condition. In [143], a modification to the fifth order WENO scheme, termed the power WENO scheme, was developed based on an extended class of limiters. Comparison with the standard WENO scheme was made with extensive numerical examples.

In our previous discussion, we did not pay attention to boundary conditions and assumed the problem has no boundary (compactly supported data or periodic boundary conditions). In practice, of course, we would need to deal with various physical boundary conditions. WENO schemes have been used for problems with different boundary conditions such as reflective (solid wall), symmetry (such as the axis in an axissymmetric setting), inflow, and outflow types. A general strategy is to define accurate ghost point values based on the specific type of boundary conditions, coupled with local characteristic decompositions. One-sided WENO approximations or reconstructions, which avoid using information from outside the computational domain, may also be used [142, 25].

3.5.5. Staggered Mesh, Multidimensional Meshes, and Multidomain WENO Scheme. The finite volume scheme (3.4), when discretized in time, can also be defined on a staggered mesh, resulting in a class of central schemes [115]. An advantage of such central schemes is that the numerical flux is computed in the smooth part of the reconstructed function, hence there is no need to use explicitly a monotone flux for the scalar case or a Riemann solver for the system case. WENO schemes based on the central scheme framework have been constructed in the literature, e.g., in [92, 93, 94, 131]. It seems that the central scheme framework allows the componentwise WENO reconstruction procedure to be used for less oscillatory results for third or even fourth order schemes; however, for very high order central WENO schemes, characteristic WENO reconstruction is still necessary to obtain stable results [131]. A detailed assessment of componentwise versus characteristic reconstructions in the context of central WENO schemes is given in [131].

Designing finite volume WENO schemes on multidimensional structured meshes is straightforward [146, 164]. Finite volume WENO schemes on two-dimensional unstructured meshes were designed in [50, 73, 146, 44, 45]. For three dimensions, finite volume WENO schemes on unstructured meshes were designed in [44, 45, 195]. As we mentioned in section 2.3.3, the WENO schemes in [50, 44, 45] choose the linear
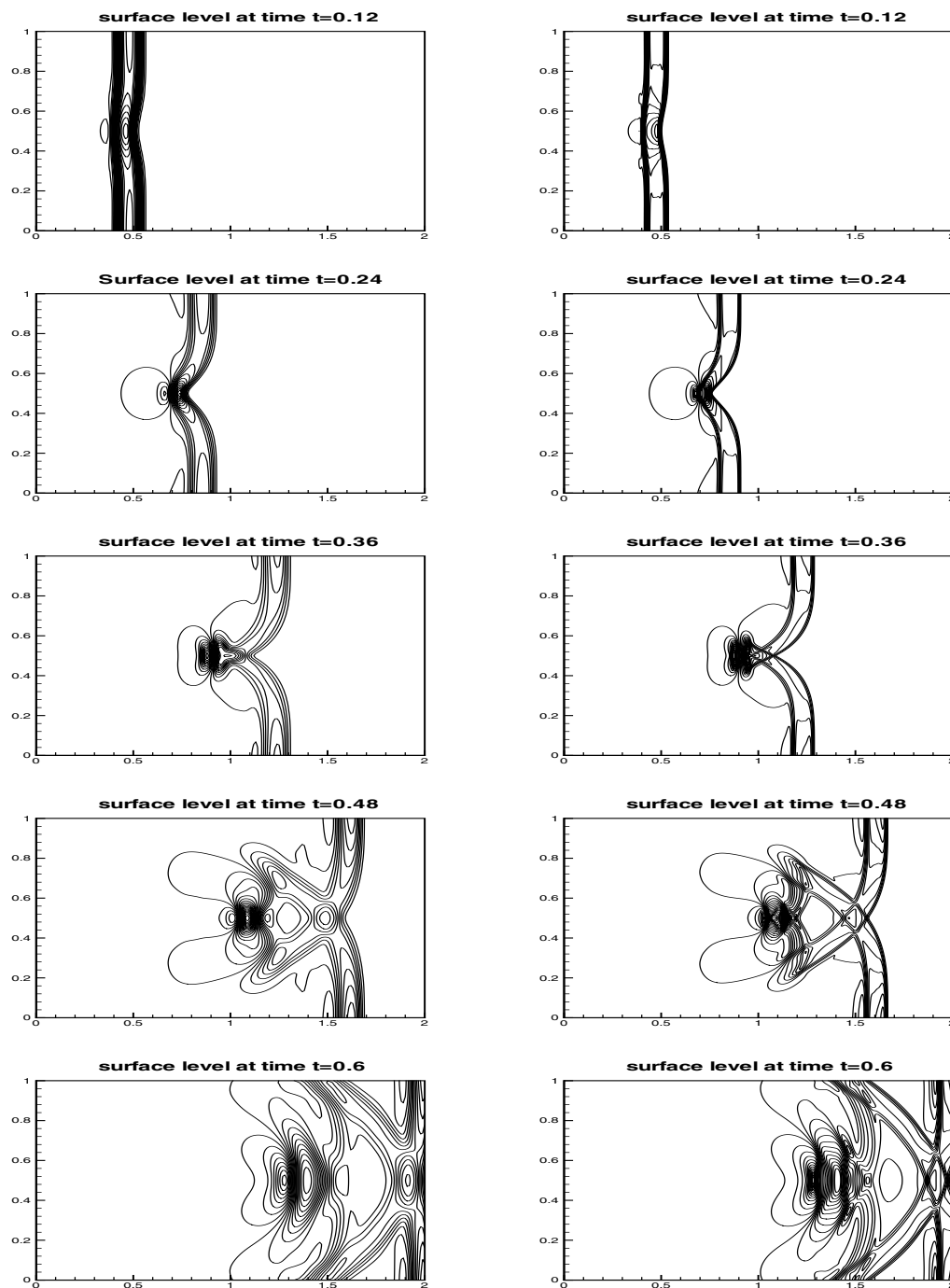
Fig. 3.2 *Reproduced from* [171]. *Two-dimensional shallow water equation. Small (1%) perturbation from still water. Well-balanced fifth order finite difference WENO scheme. The contours of the water surface level given at 30 uniformly spaced contour lines. From top to bottom: time $t = 0.12$ from 0.999703 to 1.00629; time $t = 0.24$ from 0.994836 to 1.01604; time $t = 0.36$ from 0.988582 to 1.0117; time $t = 0.48$ from 0.990344 to 1.00497; and time $t = 0.6$ from 0.995065 to 1.0056. Left: results with a 200×100 uniform mesh. Right: results with a 600×300 uniform mesh.*

weights subject only to positivity and the condition that they sum to one, without attempting to increase the order of accuracy of the approximation in each substencil. Therefore, these schemes do not achieve the optimal attainable order of accuracy for their stencil. However, these schemes are easier to design since the linear weights can be chosen to be arbitrary positive constants or to fit other constraints such as having larger linear weights for the more symmetric substencils. The WENO schemes in [73, 146, 195] follow the traditional WENO procedure to obtain approximations on the larger stencil that are of higher order accuracy than that on each substencil. Unfortunately, such schemes are very difficult to construct on unstructured meshes as the optimal linear weights depend on the local mesh distribution.

In [142], a multidomain finite difference WENO scheme is designed. The computational domain can then be generalized to any region which can be covered by overlapping patches, where for each patch a uniform Cartesian or a smooth curvilinear mesh suitable for a finite difference WENO scheme can be used. Information is transferred between patches via high order interpolation. This multidomain finite difference WENO scheme can be used in many practical situations, such as flow passing a wedge, with the cost of a finite difference scheme that is much smaller than that of a finite volume scheme. This scheme was used in [83] to study shock mitigation and drag reduction by pulsed energy lines.

3.5.6. Residual Distribution WENO Scheme. Another attempt to expand the usability of the finite difference WENO method without increasing its cost is the design of residual distribution-type finite difference WENO schemes for steady state conservation laws and convection dominated convection diffusion equations in [25, 26]. These schemes can be used on arbitrary *nonsmooth* tensor product curvilinear meshes, are conservative, and have the same cost as the usual conservative finite difference schemes for two-dimensional problems.

3.5.7. Contact Discontinuities. One difficulty of numerical solutions for conservation laws is that contact discontinuities, i.e., the discontinuities belonging to the characteristic field satisfying $\lambda'(u) \cdot r(u) \equiv 0$, where $\lambda(u)$ is an eigenvalue and $r(u)$ is the corresponding eigenvector of the Jacobian $f'(u)$ of the conservation law (3.1), are much more difficult to resolve sharply than shocks. This is because the characteristics are parallel to the discontinuity for a contact discontinuity, while they converge to the discontinuity for a shock; see Figure 3.3. Therefore, a numerical shock is usually stable with a fixed number of transition points for long time simulation, while a numerical contact discontinuity may progressively become wider for longer time simulation. Strategies to improve the resolution of contact discontinuities for high order WENO schemes include the artificial compressibility method [180, 78], subcell resolution [64, 78], and the antidiffusive flux correction method [42, 175]. In [177], the antidiffusive flux corrected WENO scheme is used to simulate the transport of a pollutant, with very good resolution.

3.5.8. Convection-Diffusion Equations and Parallel Implementation. For convection dominated convection-diffusion equations, for example, the Navier–Stokes equations with high Reynolds numbers, the WENO schemes discussed in previous subsections for conservation laws can be easily generalized. We can either use central difference approximations to the second derivative viscous terms of comparable order of accuracy, or absorb the evaluation of the viscous terms into the numerical fluxes by first computing an approximation to the first derivatives of the solution at cell interfaces to the desired order of accuracy. We refer to, e.g., [193, 196, 190, 191] for more details.
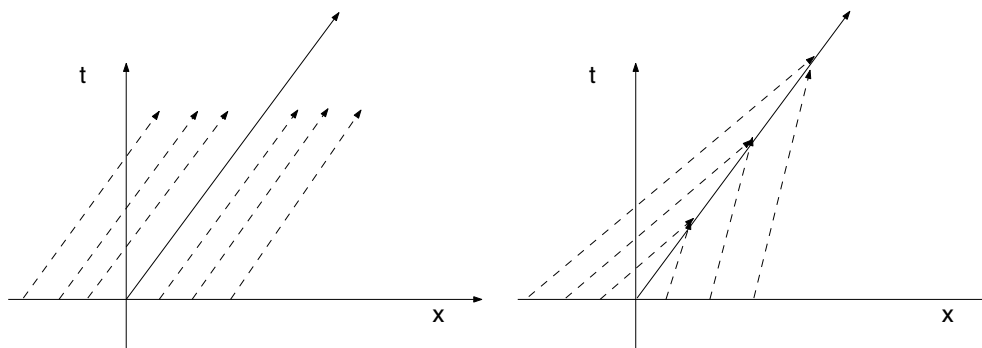
Fig. 3.3 *Characteristics. Left: contact discontinuity. Right: shock.*

Since WENO schemes are explicit schemes, they can be implemented easily on massively parallel platforms. Large-scale results obtained in, e.g., [47, 190, 191, 193, 196] were obtained using parallel WENO codes. The results in these papers indicate that the parallel efficiency of the high order WENO schemes is excellent.

4. WENO Schemes for Hamilton–Jacobi Equations. WENO schemes can also be used to solve PDEs which are not hyperbolic conservation laws. In this section we describe such an example. We consider WENO schemes for solving the following Hamilton–Jacobi equation:

$$(4.1) \qquad \varphi_t + H(\varphi_{x_1}, \ldots, \varphi_{x_d}) = 0, \qquad \varphi(x, 0) = \varphi^0(x),$$

where the Hamiltonian H is a (usually nonlinear) function that is Lipschitz continuous. H could also depend on φ, x, and t in some applications; however, the main difficulty for numerical solutions is the nonlinear dependency of H on the gradient of φ.

Hamilton–Jacobi equations appear often in many applications, for example, in control theory and differential games. General interface problems such as multiphase flow and free boundary problems are also important applications. Another important application of Hamilton–Jacobi equations is the area of image processing and computer vision.

The main difficulty in the numerical solution of the Hamilton–Jacobi equation (4.1) is that a global C^1 solution does not exist in the generic situation, regardless of the smoothness of the initial condition $\varphi^0(x)$. Singularities in the form of discontinuities in the derivatives of φ appear at a finite time in most situations, thus the solutions are Lipschitz continuous but no longer C^1. Also, such Lipschitz continuous solutions to the Hamilton–Jacobi equation (4.1) are not unique, hence we would need to approximate the physically correct "viscosity solution"; see [37]. In fact, in the one-dimensional case, there is an equivalence between the Hamilton–Jacobi equation

$$(4.2) \qquad \varphi_t + H(\varphi_x) = 0, \qquad \varphi(x, 0) = \varphi^0(x),$$

and the hyperbolic conservation law

$$(4.3) \qquad u_t + H(u)_x = 0, \qquad u(x, 0) = u^0(x),$$

if we identify $u = \varphi_x$. There is also a similar equivalence in the multidimensional case [82]. As we have seen in section 3, singularities for the conservation law (4.3) are in

the form of discontinuities in the solution u, thus u is bounded, with a bounded total variation, but is not continuous. The results for the conservation law (4.3) can be directly translated to those for the Hamilton–Jacobi equation (4.2) by integrating u once. Discontinuities in u then become discontinuities in the derivative of φ.

For the one-dimensional Hamilton–Jacobi equation (4.2), or for the multidimensional Hamilton–Jacobi equation (4.1) on a Cartesian mesh, the WENO finite difference scheme [77] can be easily designed. Such a high order WENO scheme is based on first order monotone Hamiltonians. A first order Hamiltonian $\hat{H}(u^-, u^+)$ is a nondecreasing function in its first argument u^- and a nonincreasing function in its second argument u^+, or, symbolically, $\hat{H}(\uparrow, \downarrow)$; it is consistent with the physical Hamiltonian $H(u)$, i.e., $\hat{H}(u, u) = H(u)$; and it is Lipschitz continuous with respect to both arguments u^- and u^+. Monotone Hamiltonians can also be defined for multidimensional cases (4.1). We refer to, e.g., [121] for examples of monotone Hamiltonians in one- and multidimensional cases. We now use the one-dimensional version (4.2) to demonstrate the idea of the WENO scheme, which in this case evolves the point values of the solution φ_i in the following way:

$$(4.4) \qquad\qquad \frac{d}{dt}\varphi_i + \hat{H}(u_i^-, u_i^+) = 0,$$

where $\hat{H}(u^-, u^+)$ is a monotone Hamiltonian and the values $u_i^\pm$ in (4.4) are WENO approximations to the derivatives of φ at the point x_i with a stencil one point biased to the left and one point biased to the right, respectively, as described in section 2.3.4. For example, a fifth order WENO scheme [77] uses the following stencil to approximate u_i^-:

$$S = \{x_{i-3}, x_{i-2}, x_{i-1}, x_i, x_{i+1}, x_{i+2}\}.$$

This stencil is the union of the following three substencils:

$$S_1 = \{x_{i-3}, x_{i-2}, x_{i-1}, x_i\}, \;\; S_2 = \{x_{i-2}, x_{i-1}, x_i, x_{i+1}\}, \;\; S_3 = \{x_{i-1}, x_i, x_{i+1}, x_{i+2}\}.$$

The fifth order approximation u_i^- is, as usual, a convex combination of the three third order approximations to φ_x at $x = x_i$ based on the three substencils S_1, S_2, and S_3, respectively. Time discretization of the semidiscrete scheme (4.4) can again be based on the TVD Runge–Kutta time discretizations such as (3.5).

Unlike the case of conservation laws in section 3, for the Hamilton–Jacobi equation (4.2) there is no finite volume scheme, and the finite difference scheme we described above does *not* have the restriction of uniform or smooth meshes. This finite difference scheme can be used on any mesh, smooth or not. For the multidimensional case (4.1), as long as we have a Cartesian mesh, the finite difference WENO scheme can be trivially generalized by simply computing approximations to the derivatives dimension by dimension. Thus the approximation to $u = \varphi_x$ is obtained by the one-dimensional procedure described above along the x direction with y fixed, and the approximation to $v = \varphi_y$ is obtained by the same one-dimensional procedure along the y direction with x fixed. WENO schemes can also be designed based on the central scheme framework; see, e.g., [10, 157]. However, a high order WENO scheme to solve the multidimensional case (4.1) on unstructured meshes is much more involved. We refer to [194] for the details of high order WENO schemes solving two-dimensional Hamilton–Jacobi equations on general triangulations; see also [91].

WENO schemes have been used widely in solving Hamilton–Jacobi equations coming from the level set methods [120]. For some of these application problems,

for example, for the problem of reinitialization of the signed distance function [160], one must solve steady state Hamilton–Jacobi equations repeatedly. One of the efficient methods to solve the steady state Hamilton–Jacobi equations is the so-called fast sweeping method. For high order WENO schemes, fast sweeping methods were developed recently in [197]. A common complaint about the level set method is the problem of volume (or mass) loss. However, this problem is alleviated significantly if one uses a high order scheme such as the fifth order WENO scheme in [77]. We refer to [108] for a discussion of this issue.

Similar to the difficulty associated with the resolution of contact discontinuities in conservation laws, it is also difficult to resolve corners (discontinuities in the derivative of the solution) corresponding to a linearly degenerated Hamilton–Jacobi equation. In [176], the antidiffusive flux correction technique in [175] for conservation laws is generalized to high order WENO schemes for solving Hamilton–Jacobi equations, to sharpen such corners. Numerical results in [176] demonstrate the good performance of this approach.

Finally, we mention that the convergence of a class of semi-Lagrangian large time step schemes, based on a WENO interpolation with the order of accuracy as high as 9, is proved in [14] for solving general viscosity solutions of convex Hamilton–Jacobi equations. This is the best theoretical convergence result obtained so far involving WENO schemes.

5. Relationship and Comparison with Other High Order Schemes. In this section we briefly describe a few competitive types of numerical methods for solving convection dominated problems. Rather than surveying the details of these methods, we emphasize efforts in combining the advantages of these methods and the WENO procedure. Comparisons of some of these schemes with WENO schemes can be found in [198, 151].

5.1. Discontinuous Galerkin Method. Discontinuous Galerkin methods are a class of finite element methods that have gained a lot of popularity in recent years, e.g., [32, 33, 39]. For our purpose, the discontinuous Galerkin method can also be viewed as a generalized finite volume method for solving conservation laws. For the one-dimensional conservation law (3.1), the discontinuous Galerkin method is defined as follows. Find u in the following finite-dimensional piecewise polynomial space,

$$V_{\Delta x} = \left\{ v : v|_{I_j} \in P^k(I_j), \ j = 1, \ldots, N \right\},$$

where $I_j = (x_{j-\frac{1}{2}}, x_{j+\frac{1}{2}})$ with $j = 1, \ldots, N$ is a partition of the computational domain and $P^k(I_j)$ denotes the set of polynomials of degree up to k defined on the cell I_j, such that

$$(5.1) \qquad \int_{x_{i-\frac{1}{2}}}^{x_{i+\frac{1}{2}}} u_t v \, dx - \int_{x_{i-\frac{1}{2}}}^{x_{i+\frac{1}{2}}} f(u) v_x \, dx + \hat{f}_{i+\frac{1}{2}} v_{i+\frac{1}{2}}^- - \hat{f}_{i-\frac{1}{2}} v_{i-\frac{1}{2}}^+ = 0$$

for all $v \in V_{\Delta x}$. Here $\hat{f}_{i+\frac{1}{2}} = \hat{f}(u_{i+\frac{1}{2}}^-, u_{i+\frac{1}{2}}^+)$ is a monotone numerical flux which depends on both the left and right values of u at the cell interface $x_{i+\frac{1}{2}}$. If we take $v = 1_{I_i}$ to be the indicator function of cell I_i, that is, $v(x) = 1$ when $x \in I_i$ and $v(x) = 0$ otherwise, then clearly $v \in V_{\Delta x}$ and the scheme (5.1) becomes identical

to the finite volume scheme (3.4). Therefore we may claim that the discontinuous Galerkin scheme (5.1) is a generalized finite volume scheme. However, an essential difference between the finite volume scheme (3.4) and the discontinuous Galerkin scheme (5.1) is that the finite volume scheme evolves only one piece of information per cell, namely, the cell average $\bar{u}_i$. If higher order point values $u_{i+\frac{1}{2}}^{\pm}$ are needed at the cell interfaces, they will be reconstructed by the WENO procedure. On the other hand, the discontinuous Galerkin scheme evolves the whole polynomial per cell I_i (if the polynomial is of degree k, then $k + 1$ pieces of information are evolved per cell).

Since the WENO procedure is only applied at the reconstruction stage of the finite volume scheme, it cannot be directly used within the framework of a discontinuous Galerkin scheme. Therefore, discontinuous Galerkin schemes rely on limiters to control spurious oscillations. See, e.g., [29, 28, 31].

Discontinuous Galerkin methods are more flexible than finite volume WENO schemes for solving conservation laws on multidimensional unstructured meshes. However, discontinuous Galerkin methods are less robust in dealing with solutions with strong shocks. This is because the state of the art for limiters is less advanced than the WENO procedure in controlling spurious oscillations without affecting accuracy for smooth structures.

Recently, efforts have been made in the following two directions to combine the advantages of WENO and discontinuous Galerkin schemes:

1. *The design of Hermite-type WENO schemes.* These are schemes between the finite volume WENO scheme, which evolves only one piece of information per cell, and the discontinuous Galerkin scheme, which evolves $k + 1$ pieces of information per cell for a $(k + 1)$th order method in one dimension using piecewise polynomials of degree k. The Hermite WENO schemes designed in [133, 136, 137] evolve a linear function per cell (hence they evolve two pieces of information per cell in one dimension) and reconstruct the necessary point values to higher order accuracy when necessary. Because each cell contains more than one degree of freedom, the reconstruction would involve a narrower stencil for the same order of accuracy, resulting in more compact WENO schemes.

2. *The design of WENO limiters for discontinuous Galerkin schemes.* The idea is to first identify the so-called "troubled cells," then retain only the cell average information in such cells for the purpose of conservation and use the WENO procedure to reconstruct the higher order moments of the polynomials in such cells using the information from neighboring cells. Both the traditional WENO reconstruction technique and the Hermite WENO reconstruction technique (which is more desirable since it involves a narrower stencil) can be used. This approach was pursued in [134, 133, 136]. The issue of effective "troubled cell" indicators was addressed in [135].

5.2. Compact Schemes. Compact schemes are finite difference schemes where the derivatives are approximated not by polynomial operators but by rational function operators on the discrete solutions. We refer to, e.g., [72, 89] for general discussion of compact schemes. Upwind (rather than central) compact schemes were developed in [30].

The main advantage of compact schemes is that they have better resolution power for high frequency waves than the usual finite difference schemes of the same order of accuracy. Therefore, they are especially suitable for problems involving long time evolution of waves, such as turbulence simulations [89].

Efforts have been made in the literature to develop hybrid compact WENO schemes. In [81], a compact WENO scheme is designed where the WENO procedure is used on the explicit part of the scheme. In [122], a hybrid compact WENO scheme is developed to solve shock turbulence interaction problems. A shock detector is used to find regions where the WENO approximation is used instead of the usual compact difference approximation. In [41], the WENO procedure is used to build nonlinear WENO compact schemes.

5.3. Spectral Method. For smooth problems in regular geometry, the spectral method [53, 13] is the most powerful method for obtaining accurate results, especially for long time wave propagation problems. Fourier or Chebyshev spectral methods are also very efficient because of the fast Fourier transforms. However, it is a challenge to design stable spectral schemes for solving convection dominated problems which have sharp gradient regions or shocks. Even though spectral methods with a carefully designed application of filters can produce very good results for shock wave calculations [43], such methods are not robust, in the sense that the application of filters requires experience in order to maintain stability without destroying accuracy. Another approach to designing stable spectral schemes for shock wave calculations is to add spectral vanishing viscosity [161].

Efforts have been made in the literature to develop hybrid spectral WENO schemes. In [36, 35], a hybrid spectral WENO method, using the WENO procedure near strong shocks and spectral procedure elsewhere, is developed and shown to give good numerical results for a few quite demanding test problems.

5.4. Wavelets and Multiresolution Methods. Wavelets and multiresolution methods are powerful frameworks to solve multiscale problems containing a wide range of physical scales. In applications to solve convection dominated PDEs, the multiresolution framework of Harten [65] is particularly attractive, since it utilizes the essential ideas of wavelets in their effective multiresolution decomposition in combination with features in conservative schemes for hyperbolic conservation laws relying on high order reconstruction. There have been numerous works since then combining Harten's multiresolution framework with high order, high resolution schemes; see, for example, [9, 24]. Recently, this multiresolution framework has also been combined with the WENO procedure in [11] to produce an adaptive multiresolution WENO scheme for solving conservation laws.

5.5. Dispersion Optimized Finite Difference Schemes. For application problems in which waves must propagate over a long time with a relatively coarse mesh (that is, the number of grid points per wave is not large), such as problems in aeroacoustics and electromagnetism, it is important to maintain the phase accuracy of the waves to the best extent possible. Spectral methods are the best choice to maintain such phase accuracy. Compact schemes discussed in section 5.2 are also good choices. If one must use explicit finite difference schemes, then there is a systematic approach [162] to modify the coefficients of the finite difference approximation, with the objective of increasing the phase resolution (dispersion relation) at the price of lowering the order of accuracy for the same stencil. Even though such dispersion optimized finite difference schemes are less accurate for asymptotically small mesh sizes (that is, when the number of points per wave is large), they are better than the usual finite difference schemes on the same stencil for marginally resolved waves (that is, when the number of points per wave is small).

Even though WENO schemes are nonlinear, they can also be adapted by such dispersion optimized techniques to enhance their resolution power for marginally resolved waves. Efforts are made in the literature [102, 126, 169, 111] to design such dispersion optimized WENO schemes and to apply them to turbulence simulations.

5.6. Third Order Nonoscillatory Schemes. In [105], Liu and Osher developed a class of third order nonoscillatory schemes in one space dimension, for which they proved the maximum principle and nonoscillatory properties. These schemes were generalized to two space dimensions by Noelle [116] and Kurganov and Petrova [84]. Comparing with WENO schemes, these third order nonoscillatory schemes have the advantage when a strict maximum principle is desired, such as a volume ratio calculation which should not go outside the range of $[0, 1]$. However, it seems difficult to generalize such nonoscillatory schemes to higher than third order accuracy.

6. Applications. The WENO schemes discussed in previous sections have been used in many physical and engineering applications. In this section we briefly summarize some of these applications with the objective of giving a glimpse of the diversity of possible applications of the WENO methodology, rather than providing an exhaustive list. Most of these applications have a common feature: they are solving for solutions with both discontinuities or sharp gradient regions and complicated smooth region structures.

6.1. Computational Fluid Dynamics. The largest application area of WENO schemes is the area of computational fluid dynamics (CFD). Besides the applications already mentioned in previous sections, we mention as additional examples the following representative works.

1. Shock vortex interaction is an important physical process for sound generation, and it is a simple model for shock turbulence interaction. This problem has complicated solutions where shocks of various strengths and vorticity flows coexist, which makes it ideal to be simulated by high order WENO schemes. Many papers in the literature use WENO schemes to study the details of shock vortex interactions in different physical setups and regimes, for example, [59, 123, 124, 138, 190, 191]. See also related work in blast wave/vortex interaction and sound generation in [22]; shock wave–thermal inhomogeneity interactions in [60]; reflected shock/vortex interaction near an open-ended duct in [97]; and shock/vortex interactions induced by blast waves in [98]. As an example of shock vortex interaction, in Figure 6.1 we plot the shadowgraphs (contours of $\nabla^2 \rho$ where ρ is the density) of an oblique Mach 1.2 shock with a strong colliding vortex pair simulated by the fifth order WENO scheme for the compressible Navier–Stokes equations [191]. We can see clearly that the complicated flow structure from the shock vortex interaction is resolved well by the fifth order WENO scheme.

2. High speed and turbulent flows typically contain both strong shocks and complicated flow structures, making WENO schemes good simulation tools for them. Supersonic jet and shear layers are studied in [23]. Turbulent flows in high speed aerodynamics are studied in [62]. Turbulence spectra characteristics for direct and large eddy simulations are studied in [86]. Hypersonic aerodynamic heating predictions are made in [88]. The starting process in a supersonic nozzle is studied in [114]. Direct numerical simulation and analysis of a spatially evolving supersonic turbulent boundary layer at M = 2.25 are performed in [125]. Instability wave generation and propagation in su-
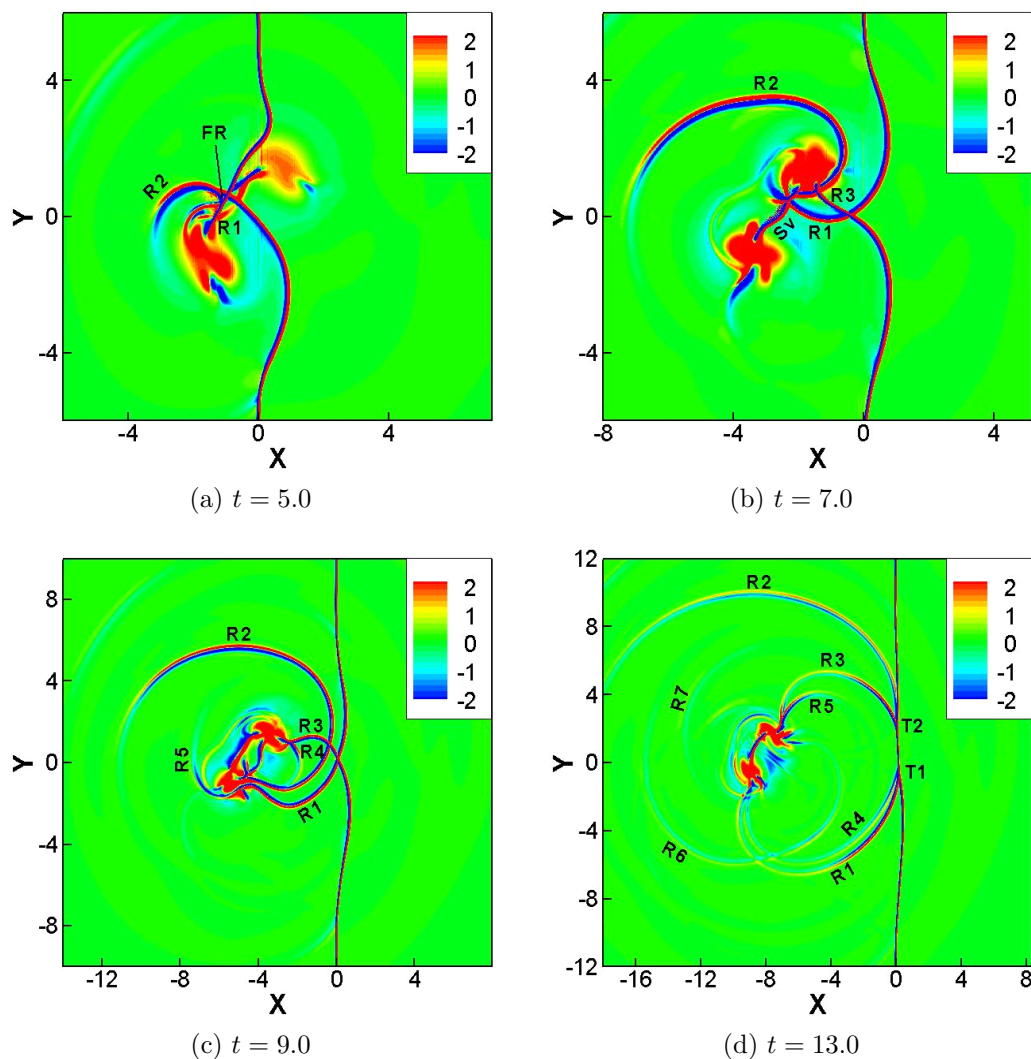
(a) $t = 5.0$

(b) $t = 7.0$

(c) $t = 9.0$

(d) $t = 13.0$

Fig. 6.1 *Reproduced from* [191]. *Fifth order WENO simulation of the evolution of an oblique shock and a colliding vortex pair interaction. Shock Mach number $M_s = 1.2$, vortex Mach number $M_\nu = 0.8$, and angle of the oblique shock wave $\alpha = 45°$.*

personic boundary layers are studied in [80]. Large eddy simulation of the shock wave and boundary layer interaction is performed using the hybrid compact/WENO scheme in [163]. Implicit WENO schemes for the compressible and incompressible Navier–Stokes equations are developed in [181, 182] and used to perform the three-dimensional wing flow computations in [183]. Computation of a supersonic turbulent flowfield with transverse injection is performed in [159]. The stochastic piston problem is studied in [101]. Nearly incompressible, inviscid Taylor–Green vortex flow is studied in [152].

3. Reacting flows, detonations, and flames contain multiple scales in the solution together with shocks, making their numerical simulation very difficult. WENO schemes have been successfully used for such simulations. Reacting
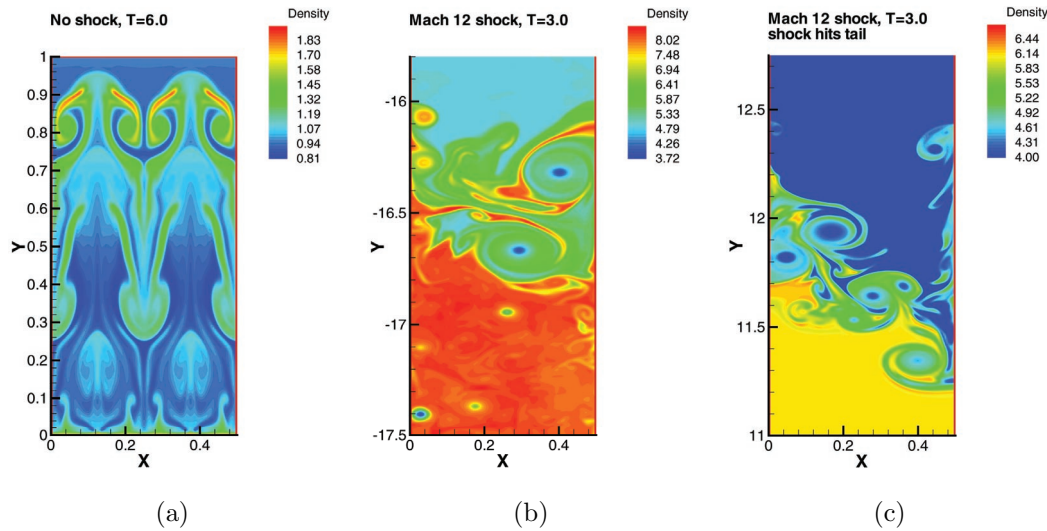
Fig. 6.2 *Reproduced from* [196]. *Ninth order WENO simulation of the Rayleigh–Taylor instability with or without shock waves. Left* (a): *the Rayleigh–Taylor flow at $T = 6.0$. Middle* (b): *Mach* 12 *shock hitting the Rayleigh–Taylor interface from the top, $T = 3.0$. Right* (c): *Mach* 12 *shock hitting the Rayleigh–Taylor interface from the bottom, $T = 3.0$. Density ρ.*

flows with complicated solution structure are studied in [2]. Pulse detonation engine phenomena are studied in [69]. A very accurate simulation of pulsating one-dimensional detonations is performed in [70, 71]. The structure and evolution of a two-dimensional H-2/O-2/Ar cellular detonation are studied in [74]. A unified model for the prediction of laminar flame transfer functions is built and comparisons are made between conical and V-flame dynamics in [141]. Modeling tools for the prediction of premixed flame transfer functions are studied in [140].

4. An interesting application of shock mitigation and drag reduction by pulsed energy lines for supersonic flows past a wedge is studied in [83] using the multidomain finite difference WENO scheme developed in [142]. The simulation results indicate a saving of energy (energy gained is larger than energy spent to generate the pulsed energy lines) for all studied configurations.

5. A WENO finite difference scheme for solving magnetohydrodynamic (MHD) flows is developed in [79]. This code is used in, e.g., [170] to study the dynamical evolution of coherent structures in intermittent two-dimensional MHD turbulence.

6. Real gas computation using an energy relaxation method is performed in [113]. Compressible multicomponent flows are simulated in [107, 110]. A pseudocompressibility method for the numerical simulation of incompressible multifluid flows is developed in [119]. Modeling and simulation for a particle-fluid two phase flow problem are studied in [188].

7. Hydrodynamic and quasi-neutral approximations for collisionless two-species plasmas are performed in [85]. Effects of shock waves on Rayleigh–Taylor instability are studied in [196]. An example of the Rayleigh–Taylor instability with or without shock waves is shown in Figure 6.2, in which a Rayleigh–Taylor flow (left picture) is compared with the flow of a Mach 12 shock hitting

the Rayleigh–Taylor interface from the top (middle picture) and from the bottom (right picture) [196]. The simulation is performed by a ninth order WENO scheme, which seems to resolve the complicated flow structures in the presence of strong shocks very well. We can clearly observe that the shock waves do speed up the transition of the Rayleigh–Taylor flow to full instability in each case.

8. Shallow water equations and sediment transport equations are studied in [38]. Two-dimensional shallow water equations are simulated by composite schemes (for which WENO is a component) in [104]; see also [103]. Underwater blast-wave focusing is studied in [96]. Nonbreaking and breaking solitary wave run-up is studied in [95]. See also [168, 171, 173, 174] for well-balanced high order WENO schemes for the shallow water equations.

9. Numerical simulation of interphase mass transfer with the level set approach is performed in [179]. Migrating and dissolving liquid drops are studied in [7, 8]. For flows in liquid helium, nonlinear effects and shock formation in the focusing of a spherical acoustic wave are studied in [4].

10. A WENO scheme is designed in [17] for the Lifshitz–Slyozov system, which models the formation of a new phase in solid mechanics. This is not exactly fluid mechanics, but the type of PDEs and difficulties in their numerical solutions are similar.

11. Several different discretization techniques are studied and compared in [99] for the transport and diffusion equations in chemical engineering problems. WENO schemes are found to be efficient and essential for numerical schemes which use a relatively small number of mesh points. In [100], WENO schemes are applied to solve the population balance equations in chemical engineering and are found to be accurate and economical for this application.

12. A careful numerical study is performed in [147] for Euler equations and in [193] for Navier–Stokes equations to demonstrate that for flow problems containing both shocks and complicated smooth region structures, it is more economical to use high order WENO schemes than to use lower order schemes to achieve the same level of resolution. See also [185] for a comparison of schemes (including the WENO scheme) for the resolution of contact discontinuity layers, in which the WENO schemes performed nicely.

6.2. Astronomy and Astrophysics. Applications in astronomy and astrophysics are closely related to those in fluid dynamics described in the previous subsection. This is because many models in astronomy and astrophysics (hydrodynamic, radiative transfer, etc.) are very similar to those in fluid dynamics. We mention in particular the following applications in which WENO schemes were successfully used.

1. A hybrid cosmological WENO hydrodynamic/N-body code is developed in [47] and applied to many astrophysical phenomena in, e.g., [46, 76, 68]. In particular, the high resolution power and small numerical viscosity of the WENO code allow the authors to study turbulence-like behavior for the low-redshift cosmic baryon fluid on large scales in [68]. A relativistic adaptive mesh refinement WENO hydrodynamics code (RAM) is developed in [192].

2. Dynamical response of a stellar atmosphere to pressure perturbations is studied in [40].

3. The radiative transfer and ionized sphere at reionization are studied in [130, 128].

4. The boundary layer between a white dwarf and its accretion disk is studied using a numerical code based on WENO ideas in [49].

5. Numerical simulation of high Mach number astrophysical jets with radiative cooling is performed in [61]. Because of the very high Mach number shock (Mach = 80) involved in the simulation, many high resolution schemes become unstable but the WENO code is able to resolve the solution well.

6.3. Semiconductor Device Simulation. WENO schemes have been used to solve various models in semiconductor device simulations. The earlier studies were mostly of moment models such as the hydrodynamic and energy transport models; however, more recent study has been focused on solving kinetic-type models such as the BGK-Poisson and Boltzmann–Poisson models. We mention in particular the following representative works. WENO schemes again show their robustness in such simulations, especially when the grid is very coarse (due to computer storage and speed limitations because of the high dimensions in the models), and hence the solution variation between neighboring grids is large in certain regions. Traditional schemes often fail or perform poorly for such coarse meshes even though they are stable for more refined meshes. The advantage of the WENO schemes is thus in its stability and resolution power on such coarse meshes.

1. A WENO solver is designed for solving the Boltzmann–Poisson system in semiconductor device simulations in [15, 16]. In its most general context, this system involves a transport equation with collision source terms in three space dimensions, three phase velocity dimensions, plus time $(6 + 1$ dimensions), coupled with a Poisson equation in three space dimensions. A direct simulation of this full system is still very difficult, if not impossible, even on today's most powerful parallel computers. A dominant simulation tool for such systems is the direct simulation Monte Carlo (DSMC) method. Even though DSMC is relatively easy to code and to use, it produces noisy results and also finds it difficult to generate probability density functions, especially in a time-dependent dynamic setting. Because of the good resolution power and nonlinear stability of the WENO algorithm, the WENO solver can be applied to devices with two space dimensions and three phase velocity dimensions, plus time, using a coarse mesh on a single PC, obtaining results which compare well with DSMC results [16]. The advantage of this WENO solver over the traditional Monte Carlo simulations include the noise-free resolution and the ability to produce the probability density functions in the dynamic regime.

2. A WENO scheme is used in [20] for the simulation and comparison of kinetic (BGK relaxation model), hydrodynamic, and high field models for semiconductor devices. It is also used to numerically verify the Child–Langmuir limit for semiconductor devices in [12].

6.4. Traffic Flows. Traffic flows are often modeled by hyperbolic-type PDEs. WENO schemes have been successfully used in the following traffic flow applications.

1. A finite difference WENO scheme is designed in [186] for a multiclass Lighthill–Whitham–Richards traffic flow model. An extension of the multiclass traffic flow model to an inhomogeneous highway, involving x-dependent fluxes which may be discontinuous in x (the physical location), is studied in [187].
The traffic flow model in [186] is a large system of hyperbolic conservation laws. The number of equations in this system is the number of different classes of drivers, which is taken to be as large as nine in the simulation in [186]. For this system, it is difficult to explicitly construct the exact Riemann solver. Instead, one typically uses an approximate Riemann solver such as the Lax–
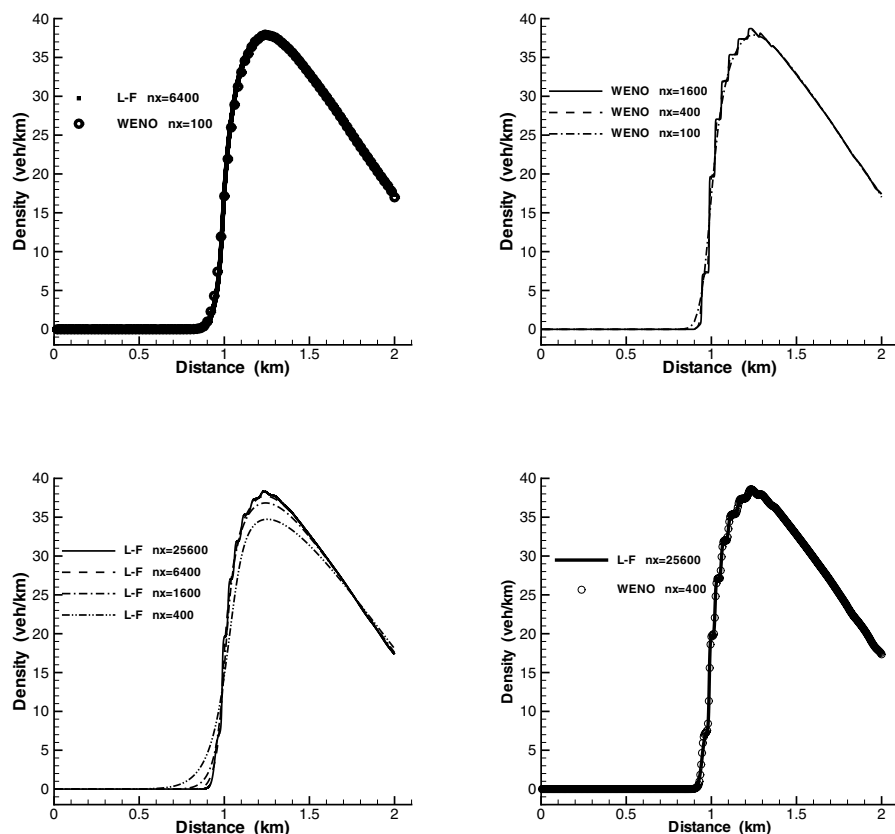
Fig. 6.3 *Reproduced from* [186]. *9-class traffic flow model. Density versus distance. Top left: comparison between the first order Lax–Friedrichs scheme with 6400 points (solid line) and the fifth order WENO scheme with 100 points (circles). Top right: convergence of the fifth order WENO scheme with 100 points (dash-dot line), 400 points (dashed line), and 1600 points (solid line). Bottom left: convergence of the first order Lax–Friedrichs scheme with 400 points (dash-double dots line), 1600 points (dash-dot line), 6400 points (dashed line), and 25600 points (solid line). Bottom right: comparison between the first order Lax–Friedrichs scheme with 25600 points (solid line) and the fifth order WENO scheme with 400 points (circles).*

Friedrichs solver. In the top left picture in Figure 6.3, we plot the numerical solution of traffic density of the first order Lax–Friedrichs scheme with 6400 grid points and of the fifth order WENO scheme with 100 grid points. If we only used the first order Lax–Friedrichs scheme in the simulation, we might be satisfied with a grid refinement study using 400, 800, 1600, 3200, and 6400 grid points, since 6400 points sounds plenty. However, the numerically converged solution for this problem contains nine small staircases and can be seen in the top right picture in Figure 6.3 (the one with 1600 grid points of the fifth order WENO scheme, which basically agrees with the result using 400 grid points of the fifth order WENO scheme). From the bottom left picture in Figure 6.3, we can see that the first order Lax–Friedrichs scheme also slowly converges to the staircase solution, but it needs as many as 25600 grid points

to achieve a resolution comparable to the fifth order WENO scheme with 400 grid points. This is a very good example to demonstrate the power of high order schemes: if one uses only the first order scheme, important solution features (the stairs) might be missed completely since the simulation might be stopped prematurely with a 6400 point grid, which would seem to be refined enough. Also, from a computational efficiency point of view, it is much more economical to use the fifth order WENO scheme with 400 points to achieve the same resolution as the first order scheme with 25600 points.

2. A reactive dynamic user equilibrium model for pedestrian flow using a continuum modeling approach is constructed in [75]. A two-dimensional walking facility that is represented as a continuum within which pedestrians can freely move in any direction is considered. The pedestrian density, flow flux, and walking speed are governed by the conservation equation. A general speed-flow-density relationship is considered. The problem is formulated by the flow conservation equation, which is a time-dependent conservation law, coupled with a static Hamilton–Jacobi equation at each fixed time t. An efficient and stable discretization for these coupled PDEs is designed in [75] using the high order WENO schemes for both the flow conservation law and the static Hamilton–Jacobi equation. Accelerating techniques such as the fast sweeping method for solving the static Hamilton–Jacobi equation are used.

6.5. Computational Biology. Many problems in computational biology involve models which are hyperbolic or otherwise convection dominated. We mention the following applications where WENO schemes were developed and used.

1. A high order, well-balanced WENO finite difference scheme is designed in [48] to study a hyperbolic model describing chemosensitive movement, in which cells change their direction reacting to the presence of a chemical substance, approaching chemically favorable environments and avoiding unfavorable ones. The high order WENO method gave much better resolution than lower order methods in demonstrating formation of networks in the hyperbolic models similar to those observed in experiments.

2. A hydrodynamic model to describe an open ionic channel flow is developed in [21]. This model is a hyperbolic conservation law system with heat conduction terms and source relaxation terms coupled with a Poisson equation. A high order ENO solver is used in [21], and followup work is performed using a WENO solver. The high order ENO/WENO solver provides an efficient tool to study the details of ionic channel flows.

3. A high order WENO scheme is designed for a hierarchical size-structured population model with nonlinear growth, mortality, and reproduction rates in [145], following up on the work in [144] in which stability and convergence are proved for a second order TVD-type high resolution scheme. The hierarchical structured population model describes population dynamics in which the size of an individual determines its access to resources and hence to its growth or decay. The model relies on a global nonlinear environment function and also has a boundary condition involving the global nonlinear function of the solution. This makes it difficult to design stable and accurate numerical schemes. As for traditional conservation laws, the solutions to this hierarchical size-structured population model also contain discontinuities. The high order WENO scheme developed in [145] can obtain much more accurate results than the second order scheme in [144] for the same meshes.

6.6. Non-PDE Applications. Since the central idea of WENO schemes is an approximation procedure, not directly related to PDEs, WENO can also be used in many non-PDE applications. We will mention in this section two such applications in computer vision and image processing.

1. The WENO interpolation is studied in a multiresolution framework for the compression of images in [5]; see also [3]. It is found that the WENO interpolation technique shows its advantage for images with edges and geometric structures.

2. A geometrically based ENO interpolation procedure using lines, circular arcs, and Euler spirals to accurately describe curves with singularities is developed in [156], resulting in accurate subpixel interpolation for curves with orientation discontinuities. WENO is expected to yield similar or improved results.

7. Concluding Remarks. We have given a review of the algorithm design, analysis, implementation, and application of high order WENO schemes for solving convection dominated problems. The extensive list of applications mentioned in this paper, or contained in the references and their references, will hopefully convince the reader of the wide applicability of WENO schemes. We mention in this last section a few topics concerning WENO schemes which are currently being investigated.

1. Efficient and robust implicit time discretization involving WENO spatial discretizations. This would be helpful for situations with significant diffusion in some regions for a convection-diffusion equation, or in an adaptive environment where the grid size might be very small in some regions. It would also be useful for computing steady state solutions. The difficulty here is the high level of nonlinearity in the nonlinear weights. For a fully implicit discretization, the resulting nonlinear system at each iteration is costly to solve, and certain iterative procedures such as Newton's method do not seem to be robust near strong shocks for a large time step [55]. Preliminary investigation of the possibility of freezing some of the nonlinear weights in the time discretization was made in [57]. More study is needed to obtain a robust and efficient approach for multidimensional systems containing strong shocks.

2. Different designs of nonlinear weights for specific purposes. Examples of such designs include the modified nonlinear weights to enhance accuracy in smooth regions, especially at smooth extrema [70], discussed in section 2.3.5; the modified weights to improve steady state convergence [189], discussed in section 2.3.5; and the dispersion optimized WENO schemes [102, 126, 169, 111], discussed in section 5.5. It can be imagined that different design of the nonlinear weights tailored toward specific classes of problems would enhance the accuracy, stability, and other good properties of the WENO scheme.

3. While WENO schemes on structured (either Cartesian or smooth curvilinear) meshes are quite mature, the development of WENO schemes on unstructured meshes is less advanced; see section 3.5.5. In particular, simple, efficient, and robust WENO schemes for unstructured meshes in three dimensions still require a lot of investigation; see the preliminary results in [44, 45, 195].

4. The hybridizing of the WENO methodology with other types of schemes, such as the WENO compact schemes discussed in section 5.2, the hybrid WENO spectral scheme discussed in section 5.3, and the WENO scheme within a multiresolution framework discussed in section 5.4, has the potential of producing schemes maintaining the advantages of both the WENO schemes and other types of schemes and is worthy of further investigation. The applica-

tion of the WENO methodology to other schemes, such as using WENO as a
limiter for the discontinuous Galerkin method discussed in section 5.1, is also
a promising research direction.

5. The design of WENO schemes with special properties for specific applica-
tions, such as the well-balanced WENO schemes discussed in section 3.5.3,
will significantly enhance the applicability of WENO schemes to these spe-
cific applications. Along a similar line, one could imagine designing WENO
schemes which are uniformly accurate and stable for stiff perturbations from
equilibriums.

6. The design of WENO schemes based on building blocks which are not polyno-
mials would be beneficial. Polynomials are the simplest and in most situations
sufficiently adequate functions to use as building blocks for interpolation and
reconstruction; however, other types of functions, such as radial basis func-
tions, local exponential, and local trigonometric functions, may perform bet-
ter in some applications. ENO schemes with building blocks which are not
polynomials were designed in [27]. Discontinuous Galerkin methods with ap-
proximation spaces consisting of functions which are not polynomials were
designed in [184]. Preliminary results on using polyharmonic splines in the
WENO reconstruction on unstructured meshes were given in [1]. Further
research in this direction would be desirable.

7. Theoretical analysis of WENO schemes. While modifications to the schemes
solely for the purpose of stability or convergence analysis at the price of in-
creased computational cost or decreased quality in numerical results should be
discouraged (it should be especially discouraged if the modification destroys
the self-similarity property of the scheme; see section 3.5.1), any analysis of
the unmodulated WENO schemes, even partial results, would be valuable.
The convergence result for the Hamilton–Jacobi equations [14], reviewed in
section 4, is a good example of such analysis. It would be very interesting to
see if similar results can be proved for a reasonable WENO scheme for specific
conservation laws; see, for example, [129] for a weaker result requiring more
restrictive reconstructions.

8. Application of the WENO idea to a wider class of problems. Since the es-
sential idea of WENO is just an interpolation or reconstruction procedure
that is not directly related to PDEs, we can imagine the application of this
idea to many non-PDE areas, such as image and signal processing, computer
graphics, and data and information processing.

REFERENCES

[1] T. Aboiyar, E.H. Georgoulis, and A. Iske, *High order WENO finite volume schemes using polyharmonic spline reconstruction*, in Proceedings of the International Conference on Numerical Analysis and Approximation Theory (NAAT 2006), Cluj-Napoca, Romania, 2006, pp. 113–126.

[2] K. Alhumaizi, *Comparison of finite difference methods for the numerical simulation of reacting flow*, Comput. Chem. Engrg., 28 (2004), pp. 1759–1769.

[3] S. Amat, S. Busquier, and J.C. Trillo, *On multiresolution schemes using a stencil selection procedure: Applications to ENO schemes*, Numer. Algorithms, 44 (2007), pp. 45–68.

[4] C. Appert, C. Tenaud, X. Chavanne, S. Balibar, F. Caupin, and D. d'Humieres, *Nonlinear effects and shock formation in the focusing of a spherical acoustic wave: Numerical simulations and experiments in liquid helium*, Eur. Phys. J. B Condens. Matter. Phys., 35 (2003), pp. 531–549.

[5] F. ARÀNDIGA AND A.M. BELDA, *Weighted ENO interpolation and applications*, Commun. Nonlinear Sci. Numer. Simul., 9 (2004), pp. 187–195.

[6] D. BALSARA AND C.-W. SHU, *Monotonicity preserving weighted essentially non-oscillatory schemes with increasingly high order of accuracy*, J. Comput. Phys., 160 (2000), pp. 405–452.

[7] E. BASSANO, *Level-set based numerical simulation of a migrating and dissolving liquid drop in a cylindrical cavity*, Internat. J. Numer. Methods Fluids, 44 (2004), pp. 409–429.

[8] E. BASSANO AND D. CASTAGNOLO, *Marangoni migration of a methanol drop in cyclohexane matrix in a closed cavity*, Microgravity Sci. Technol., 14 (2003), pp. 20–33.

[9] B.L. BIHARI AND A. HARTEN, *Application of generalized wavelets: A multiresolution scheme*, J. Comput. Phys., 61 (1995), pp. 275–321.

[10] S. BRYSON AND D. LEVY, *High-order central WENO schemes for multidimensional Hamilton–Jacobi equations*, SIAM J. Numer. Anal., 41 (2003), pp. 1339–1369.

[11] R. BÜRGER AND A. KOZAKEVICIUS, *Adaptive multiresolution WENO schemes for multi-species kinematic flow models*, J. Comput. Phys., 224 (2007), pp. 1190–1222.

[12] M.J. CACERES, J.A. CARRILLO, AND P. DEGOND, *The Child–Langmuir limit for semiconductors: A numerical validation*, Math. Model. Numer. Anal., 36 (2002), pp. 1161–1176.

[13] C. CANUTO, M.Y. HUSSAINI, A. QUARTERNONI, AND T.A. ZANG, *Spectral Methods in Fluid Dynamics*, Springer-Verlag, Berlin, 1988.

[14] E. CARLINI, R. FERRETTI, AND G. RUSSO, *A weighted essentially nonoscillatory, large time-step scheme for Hamilton–Jacobi equations*, SIAM J. Sci. Comput., 27 (2005), pp. 1071–1091.

[15] J.A. CARRILLO, I.M. GAMBA, A. MAJORANA, AND C.-W. SHU, *A WENO-solver for the transients of Boltzmann–Poisson system for semiconductor devices. Performance and comparisons with Monte Carlo methods*, J. Comput. Phys., 184 (2003), pp. 498–525.

[16] J.A. CARRILLO, I. GAMBA, A. MAJORANA, AND C.-W. SHU, *2D semiconductor device simulations by WENO-Boltzmann schemes: Efficiency, boundary conditions and comparison to Monte Carlo methods*, J. Comput. Phys., 214 (2006), pp. 55–80.

[17] J.A. CARRILLO AND T. GOUDON, *A numerical study on large-time asymptotics of the Lifshitz-Slyozov system*, J. Sci. Comput., 20 (2004), pp. 69–113.

[18] M. CARSTRO, J.M. GAALLARDO, AND C. PARÉS, *High order finite volume schemes based on reconstruction of states for solving hyperbolic systems with nonconservative products. Application to shallow-water systems*, Math. Comp., 75 (2006), pp. 1103–1134.

[19] J. CASPER, C.-W. SHU, AND H.L. ATKINS, *Comparison of two formulations for high-order accurate essentially nonoscillatory schemes*, AIAA J., 32 (1994), pp. 1970–1977.

[20] C. CERCIGNANI, I. GAMBA, J. JEROME, AND C.-W. SHU, *Device benchmark comparisons via kinetic, hydrodynamic, and high-field models*, Comput. Methods Appl. Mech. Engrg., 181 (2000), pp. 381–392.

[21] D.P. CHEN, R.S. EISENBERG, J.W. JEROME, AND C.-W. SHU, *Hydrodynamic model of temperature change in open ionic channels*, Biophys. J., 69 (1995), pp. 2304–2322.

[22] H. CHEN AND S.M. LIANG, *Planar blast/vortex interaction and sound generation*, AIAA J., 40 (2002), pp. 2298–2304.

[23] T.S. CHENG AND K.S. LEE, *Numerical simulations of underexpanded supersonic jet and free shear layer using WENO schemes*, Internat. J. Heat Fluid Flow, 26 (2005), pp. 755–770.

[24] G. CHIAVASSA AND R. DONAT, *Point value multiscale algorithms for 2D compressive flows*, SIAM J. Sci. Comput., 23 (2001), pp. 805–823.

[25] C.-S. CHOU AND C.-W. SHU, *High order residual distribution conservative finite difference WENO schemes for steady state problems on non-smooth meshes*, J. Comput. Phys., 214 (2006), pp. 698–724.

[26] C.-S. CHOU AND C.-W. SHU, *High order residual distribution conservative finite difference WENO schemes for convection-diffusion steady state problems on non-smooth meshes*, J. Comput. Phys., 224 (2007), pp. 992–1020.

[27] S. CHRISTOFI, *The study of building blocks for essentially non-oscillatory (ENO) schemes*, Ph.D. thesis, Division of Applied Mathematics, Brown University, 1996.

[28] B. COCKBURN, S. HOU, AND C.-W. SHU, *The Runge-Kutta local projection discontinuous Galerkin finite element method for conservation laws IV: The multidimensional case*, Math. Comp., 54 (1990), pp. 545–581.

[29] B. COCKBURN AND C.-W. SHU, *TVB Runge-Kutta local projection discontinuous Galerkin finite element method for conservation laws II: General framework*, Math. Comp., 52 (1989), pp. 411–435.

[30] B. COCKBURN AND C.-W. SHU, *Nonlinearly stable compact schemes for shock calculations*, SIAM J. Numer. Anal., 31 (1994), pp. 607–627.

[31] B. COCKBURN AND C.-W. SHU, *The Runge-Kutta discontinuous Galerkin method for conservation laws* V: *Multidimensional systems*, J. Comput. Phys., 141 (1998), pp. 199–224.

[32] B. COCKBURN AND C.-W. SHU, *Runge-Kutta discontinuous Galerkin methods for convection-dominated problems*, J. Sci. Comput., 16 (2001), pp. 173–261.

[33] B. COCKBURN AND C.-W. SHU, *Foreword for the special issue on discontinuous Galerkin method*, J. Sci. Comput., 22-23 (2005), pp. 1–3.

[34] P. COLELLA AND P.R. WOODWARD, *The piecewise parabolic method (PPM) for gas dynamical simulations*, J. Comput. Phys., 54 (1984), pp. 174–201.

[35] B. COSTA AND W.S. DON, *Multi-domain hybrid spectral-WENO methods for hyperbolic conservation laws*, J. Comput. Phys., 224 (2007), pp. 970–991.

[36] B. COSTA, W.S. DON, D. GOTTLIEB, AND R. SENDERSKY, *Two-dimensional multi-domain hybrid spectral-WENO methods for conservation laws*, Commun. Comput. Phys., 1 (2006), pp. 548–574.

[37] M. CRANDALL AND P.L. LIONS, *Viscosity solutions of Hamilton-Jacobi equations*, Trans. Amer. Math. Soc., 277 (1983), pp. 1–42.

[38] N. CRNJARIC-ZIC, S. VUKOVIC, AND L. SOPTA, *Extension of ENO and WENO schemes to one-dimensional sediment transport equations*, Comput. & Fluids, 33 (2004), pp. 31–56.

[39] C. DAWSON, *Foreword for the special issue on discontinuous Galerkin method*, Comput. Methods Appl. Mech. Engrg., 195 (2006), p. 3183.

[40] L. DEL ZANNA, M. VELLI, AND P. LONDRILLO, *Dynamical response of a stellar atmosphere to pressure perturbations: Numerical simulations*, Astron. Astrophys., 330 (1998), pp. L13–L16.

[41] X. DENG AND H. ZHANG, *Developing high-order weighted compact nonlinear schemes*, J. Comput. Phys., 165 (2000), pp. 22–44.

[42] B. DESPRÉS AND F. LAGOUTIÈRE, *Contact discontinuity capturing schemes for linear advection and compressible gas dynamics*, J. Sci. Comput., 16 (2001), pp. 479–524.

[43] W.S. DON AND D. GOTTLIEB, *Spectral simulation of supersonic reactive flows*, SIAM J. Numer. Anal., 35 (1998), pp. 2370–2384.

[44] M. DUMBSER AND M. KÄSER, *Arbitrary high order non-oscillatory finite volume schemes on unstructured meshes for linear hyperbolic systems*, J. Comput. Phys., 221 (2007), pp. 693–723.

[45] M. DUMBSER, M. KÄSER, V.A. TITAREV, AND E.F. TORO, *Quadrature-free non-oscillatory finite volume schemes on unstructured meshes for nonlinear hyperbolic systems*, J. Comput. Phys., 226 (2007), pp. 204–243.

[46] L.-L. FENG, J. PANDO, AND L.-Z. FANG, *Intermittent features of the quasar Ly alpha transmitted flux: Results from cosmological hydrodynamic simulations*, Astrophys. J., 587 (2003), pp. 487–499.

[47] L.-L. FENG, C.-W. SHU, AND M. ZHANG, *A hybrid cosmological hydrodynamic/N-body code based on a weighted essentially non-oscillatory scheme*, Astrophys. J., 612 (2004), pp. 1–13.

[48] F. FILBET AND C.-W. SHU, *Approximation of hyperbolic models for chemosensitive movement*, SIAM J. Sci. Comput., 27 (2005), pp. 850–872.

[49] J.L. FISKER AND D.S. BALSARA, *Simulating the boundary layer between a white dwarf and its accretion disk*, Astrophys. J., 635 (2005), pp. L69–L72.

[50] O. FRIEDRICHS, *Weighted essentially non-oscillatory schemes for the interpolation of mean values on unstructured grids*, J. Comput. Phys., 144 (1998), pp. 194–212.

[51] A. GADIOU AND C. TENAUD, *Implicit WENO shock capturing scheme for unsteady flows. Application to one-dimensional Euler equations*, Internat. J. Numer. Methods Fluids, 45 (2004), pp. 197–229.

[52] S.K. GODUNOV, *A difference scheme for numerical computation of discontinuous solutions of equations of fluid dynamics*, Mat. Sb., 47 (1959), pp. 271–306.

[53] D. GOTTLIEB AND S. ORSZAG, *Numerical Analysis of Spectral Methods: Theory and Applications*, CBMS-NSF Reg. Conf. Ser. in Appl. Math. 26, SIAM, Philadelphia, 1977.

[54] D. GOTTLIEB AND C.-W. SHU, *On the Gibbs phenomenon and its resolution*, SIAM Rev., 39 (1997), pp. 644–668.

[55] S. GOTTLIEB, *Convergence to Steady-State of Weighted ENO Schemes, Norm Preserving Runge-Kutta Methods and a Modified Conjugate Gradient Method*, Ph.D. thesis, Division of Applied Mathematics, Brown University, 1998.

[56] S. GOTTLIEB, D. GOTTLIEB, AND C.-W. SHU, *Recovering high order accuracy in WENO computations of steady state hyperbolic systems*, J. Sci. Comput., 28 (2006), pp. 307–318.

[57] S. GOTTLIEB, J.S. MULLEN, AND S.J. RUUTH, *A fifth order flux implicit WENO method*, J. Sci. Comput., 27 (2006), pp. 271–287.

[58] S. Gottlieb, C.-W. Shu, and E. Tadmor, *Strong stability-preserving high-order time discretization methods*, SIAM Rev., 43 (2001), pp. 89–112.

[59] F. Grasso and S. Pirozzoli, *Shock-wave-vortex interactions: Shock and vortex deformations, and sound production*, Theoret. Comput. Fluid Dynam., 13 (2000), pp. 421–456.

[60] F. Grasso and S. Pirozzoli, *Shock wave-thermal inhomogeneity interactions: Analysis and numerical simulations of sound generation*, Phys. Fluids, 12 (2000), pp. 205–219.

[61] Y. Ha, C.L. Gardner, A. Gelb, and C.-W. Shu, *Numerical simulation of high Mach number astrophysical jets with radiative cooling*, J. Sci. Comput., 24 (2005), pp. 597–612.

[62] A. Hadjadj and A. Kudryavtsev, *Computation and flow visualization in high-speed aerodynamics*, J. Turbulence, 6 (16) (2005), pp. 1–25.

[63] A. Harten, *High resolution schemes for hyperbolic conservation laws*, J. Comput. Phys., 49 (1983), pp. 357–393.

[64] A. Harten, *ENO schemes with subcell resolution*, J. Comput. Phys., 83 (1989), pp. 148–184.

[65] A. Harten, *Multiresolution algorithms for the numerical solution of hyperbolic conservation laws*, Comm. Pure Appl. Math., 48 (1995), pp. 1305–1342.

[66] A. Harten, B. Engquist, S. Osher, and S. Chakravarthy, *Uniformly high order essentially non-oscillatory schemes*, III, J. Comput. Phys., 71 (1987), pp. 231–303.

[67] A. Harten, S. Osher, B. Engquist, and S. Chakravarthy, *Some results on uniformly high order accurate essentially non-oscillatory schemes*, Appl. Numer. Math., 2 (1986), pp. 347–377.

[68] P. He, J. Liu, L.-L. Feng, C.-W. Shu, and L.-Z. Fang, *Low-redshift cosmic baryon fluid on large scales and She-Leveque universal scaling*, Phys. Rev. Lett., 96 (2006), article 051302.

[69] X. He and A.R. Karagozian, *Numerical simulation of pulse detonation engine phenomena*, J. Sci. Comput., 19 (2003), pp. 201–224.

[70] A.K. Henrick, T.D. Aslam, and J.M. Powers, *Mapped weighted essentially non-oscillatory schemes: Achieving optimal order near critical points*, J. Comput. Phys., 207 (2005), pp. 542–567.

[71] A.K. Henrick, T.D. Aslam, and J.M. Powers, *Simulations of pulsating one-dimensional detonations with true fifth order accuracy*, J. Comput. Phys., 213 (2006), pp. 311–329.

[72] R. Hirsh, *Higher order accurate difference solutions of fluid mechanics problems by a compact differencing technique*, J. Comput. Phys., 19 (1975), pp. 90–109.

[73] C. Hu and C.-W. Shu, *Weighted essentially non-oscillatory schemes on triangular meshes*, J. Comput. Phys., 150 (1999), pp. 97–127.

[74] X.Y. Hu, D.L. Zhang, B.C. Khoo, and Z.L. Jiang, *The structure and evolution of a two-dimensional H-2/O-2/Ar cellular detonation*, Shock Waves, 14 (2005), pp. 37–44.

[75] L. Huang, S.C. Wong, M. Zhang, C.-W. Shu, and W.H.K. Lam, *Revisiting Hughes' dynamic continuum model for pedestrian flow and the development of an efficient solution algorithm*, Transport. Res. B, 43 (2009), pp. 127–141.

[76] P. Jamkhedkar, L.-L. Feng, W. Zheng, and L.-Z. Fang, *Power spectrum and intermittency of Ly alpha transmitted flux of QSO HE* 2347-4342, Astrophys. J., 633 (2005), pp. 52–60.

[77] G.-S. Jiang and D. Peng, *Weighted ENO schemes for Hamilton–Jacobi equations*, SIAM J. Sci. Comput., 21 (2000), pp. 2126–2143.

[78] G. Jiang and C.-W. Shu, *Efficient implementation of weighted ENO schemes*, J. Comput. Phys., 126 (1996), pp. 202–228.

[79] G. Jiang and C.-C. Wu, *A high order WENO finite difference scheme for the equations of ideal magnetohydrodynamics*, J. Comput. Phys., 150 (1999), pp. 561–594.

[80] L. Jiang, M. Choudhari, C.L. Chang, and C.Q. Liu, *Direct numerical simulations of instability-wave generation and propagation in supersonic boundary layers*, in Wave Phenomena in Physics and Engineering: New Models, Algorithms, and Applications, Lecture Notes in Comput. Sci. 2668, Springer-Verlag, Berlin, 2003, pp. 859–870.

[81] L. Jiang, H. Shan, and C.Q. Liu, *Weighted compact scheme for shock capturing*, Internat. J. Comput. Fluid Dynam., 15 (2001), pp. 147–155.

[82] S. Jin and Z. Xin, *Numerical passage from systems of conservation laws to Hamilton–Jacobi equations, and relaxation schemes*, SIAM J. Numer. Anal., 35 (1998), pp. 2385–2404.

[83] K. Kremeyer, K. Sebastian, and C.-W. Shu, *Computational study of shock mitigation and drag reduction by pulsed energy lines*, AIAA J., 44 (2006), pp. 1720–1731.

[84] A. Kurganov and G. Petrova, *A third-order semi-discrete genuinely multidimensional central scheme for hyperbolic conservation laws and related problems*, Numer. Math., 88 (2001), pp. 683–729.

[85] S. Labrunie, J.A. Carrillo, and P. Bertrand, *Numerical study on hydrodynamic and quasi-neutral approximations for collisionless two-species plasmas*, J. Comput. Phys., 200 (2004), pp. 267–298.

[86] F. Ladeinde, X.D. Cai, M.R. Visbal, and D.V. Gaitonde, *Turbulence spectra characteristics of high order schemes for direct and large eddy simulation*, Appl. Numer. Math., 36 (2001), pp. 447–474.

[87] P. Lax and M. Mock, *The computation of discontinuous solutions of linear hyperbolic equations*, Comm. Pure Appl. Math., 31 (1978), pp. 423–430.

[88] T.K. Lee, X.L. Zhong, L. Gong, and R. Quinn, *Hypersonic aerodynamic heating prediction using weighted essentially nonoscillatory schemes*, J. Spacecraft Rockets, 40 (2003), pp. 294–298.

[89] S. Lele, *Compact finite difference schemes with spectral-like resolution*, J. Comput. Phys., 103 (1992), pp. 16–42.

[90] R.J. LeVeque, *Numerical Methods for Conservation Laws*, Birkhäuser Verlag, Basel, 1990.

[91] D. Levy, S. Nayak, C.-W. Shu, and Y.-T. Zhang, *Central WENO schemes for Hamilton–Jacobi equations on triangular meshes*, SIAM J. Sci. Comput., 28 (2006), pp. 2229–2247.

[92] D. Levy, G. Puppo, and G. Russo, *Central WENO schemes for hyperbolic systems of conservation laws*, M2AN Math. Model. Numer. Anal., 33 (1999), pp. 547–571.

[93] D. Levy, G. Puppo, and G. Russo, *Compact central WENO schemes for multidimensional conservation laws*, SIAM J. Sci. Comput., 22 (2000), pp. 656–672.

[94] D. Levy, G. Puppo, and G. Russo, *A third order central WENO scheme for 2D conservation laws*, Appl. Numer. Math., 33 (2000), pp. 415–421.

[95] Y. Li and F. Raichlen, *Non-breaking and breaking solitary wave run-up*, J. Fluid Mech., 456 (2002), pp. 295–318.

[96] S. Liang and H. Chen, *Numerical simulation of underwater blast-wave focusing using a high-order scheme*, AIAA J., 37 (1999), pp. 1010–1013.

[97] S.M. Liang, W.T. Chung, H. Chen, and S.H. Shyu, *Numerical investigation of reflected shock/vortex interaction near an open-ended duct*, AIAA J., 43 (2005), pp. 349–356.

[98] S.M. Liang and C.P. Lo, *Shock/vortex interactions induced by blast waves*, AIAA J., 41 (2003), pp. 1341–1346.

[99] Y.I. Lim, J.M. Le Lann, and X. Joulia, *Accuracy, temporal performance and stability comparisons of discretization methods for the numerical solution of partial differential equations (PDEs) in the presence of steep moving fronts*, Comput. Chem. Engrg., 25 (2001), pp. 1483–1492.

[100] Y.I. Lim, J.M. Le Lann, X.M. Meyer, X. Joulia, G. Lee, and E.S. Yoon, *On the solution of population balance equations (PBE) with accurate front tracking methods in practical crystallization processes*, Chem. Engrg. Sci., 57 (2002), pp. 3715–3732.

[101] G. Lin, C.H. Su, and G.E. Karniadakis, *The stochastic piston problem*, Proc. Natl. Acad. Sci. USA, 101 (2004), pp. 15840–15845.

[102] S.Y. Lin and J.J. Hu, *Parametric study of weighted essentially nonoscillatory schemes for computational aeroacoustics*, AIAA J., 39 (2001), pp. 371–379.

[103] R. Liska and B. Wendroff, *Composite schemes for conservation laws*, SIAM J. Numer. Anal., 35 (1998), pp. 2250–2271.

[104] R. Liska and B. Wendroff, *Two-dimensional shallow water equations by composite schemes*, Internat. J. Numer. Methods Fluids, 30 (1999), pp. 461–479.

[105] X.-D. Liu and S. Osher, *Nonoscillatory high order accurate self-similar maximum principle satisfying shock capturing schemes I*, SIAM J. Numer. Anal., 33 (1996), pp. 760–779.

[106] X.-D. Liu, S. Osher, and T. Chan, *Weighted essentially non-oscillatory schemes*, J. Comput. Phys., 115 (1994), pp. 200–212.

[107] B. Lombard and R. Donat, *The explicit simplified interface method for compressible multicomponent flows*, SIAM J. Sci. Comput., 27 (2005), pp. 208–230.

[108] F. Losasso, R. Fedkiw, and S. Osher, *Spatially adaptive techniques for level set methods and incompressible flow*, Comput. & Fluids, 35 (2006), pp. 995–1010.

[109] A. Majda and S. Osher, *Propagation of error into regions of smoothness for accurate difference approximations to hyperbolic equations*, Comm. Pure Appl. Math., 30 (1977), pp. 671–705.

[110] A. Marquina and P. Mulet, *A flux-split algorithm applied to conservative models for multicomponent compressible flows*, J. Comput. Phys., 185 (2003), pp. 120–138.

[111] M.P. Martin, E.M. Taylor, M. Wu, and V.G. Weirs, *A bandwidth-optimized WENO scheme for the direct numerical simulation of compressible turbulence*, J. Comput. Phys., 220 (2006), pp. 270–289.

[112] B. Merryman, *Understanding the Shu-Osher conservative finite difference form*, J. Sci. Comput., 19 (2003), pp. 309–322.

[113] P. Montarnal and C.-W. Shu, *Real gas computation using an energy relaxation method and high order WENO schemes*, J. Comput. Phys., 148 (1999), pp. 59–80.

[114] A.S. MOURONVAL AND A. HADJADJ, *Numerical study of the starting process in a supersonic nozzle*, J. Propulsion Power, 21 (2005), pp. 374–378.

[115] H. NESSYAHU AND E. TADMOR, *Non-oscillatory central differencing for hyperbolic conservation laws*, J. Comput. Phys., 87 (1990), pp. 408–463.

[116] S. NOELLE, *A comparison of third and second order accurate finite volume schemes for the two-dimensional compressible Euler equations*, in Proceedings of the 7th International Conferences on Hyperbolic Problems, Zürich, 1998, Internat. Ser. Numer. Math. 129, Birkhäuser, Basel, 1998, pp. 757–766.

[117] S. NOELLE, N. PANKRATZ, G. PUPPO, AND J.R. NATVIG, *Well-balanced finite volume schemes of arbitrary order of accuracy for shallow water flows*, J. Comput. Phys., 213 (2006), pp. 474–499.

[118] S. NOELLE, Y. XING, AND C.-W. SHU, *High order well-balanced finite volume WENO schemes for shallow water equation with moving water*, J. Comput. Phys., 226 (2007), pp. 29–58.

[119] R.R. NOURGALIEV, T.N. DINH, AND T.G. THEOFANOUS, *A pseudocompressibility method for the numerical simulation of incompressible multifluid flows*, Internat. J. Multiphase Flow, 30 (2004), pp. 901–937.

[120] S. OSHER AND R. FEDKIW, *Level Set Methods and Dynamic Implicit Surfaces*, Springer-Verlag, New York, 2003.

[121] S. OSHER AND C.-W. SHU, *High-order essentially nonoscillatory schemes for Hamilton–Jacobi equations*, SIAM J. Numer. Anal., 28 (1991), pp. 907–922.

[122] S. PIROZZOLI, *Conservative hybrid compact-WENO schemes for shock-turbulence interaction*, J. Comput. Phys., 178 (2002), pp. 81–117.

[123] S. PIROZZOLI, *Dynamics of ring vortices impinging on planar shock waves*, Phys. Fluids, 16 (2004), pp. 1171–1185.

[124] S. PIROZZOLI, F. GRASSO, AND A. D'ANDREA, *Interaction of a shock wave with two counter-rotating vortices: Shock dynamics and sound production*, Phys. Fluids, 13 (2001), pp. 3460–3481.

[125] S. PIROZZOLI, F. GRASSO, AND T.B. GATSKI, *Direct numerical simulation and analysis of a spatially evolving supersonic turbulent boundary layer at $M = 2.25$*, Phys. Fluids, 16 (2004), pp. 530–545.

[126] D. PONZIANI, S. PIROZZOLI, AND F. GRASSO, *Development of optimized weighted-ENO schemes for multiscale compressible flows*, Internat. J. Numer. Methods Fluids, 42 (2003), pp. 953–977.

[127] G. PUPPO AND G. RUSSO, *Staggered finite difference schemes for conservation laws*, J. Sci. Comput., 27 (2006), pp. 403–418.

[128] J.-M. QIU, L.-L. FENG, C.-W. SHU, AND L.-Z. FANG, *A WENO algorithm of the temperature and ionization profiles around a point source*, New Astronomy, 12 (2007), pp. 398–409.

[129] J.-M. QIU AND C.-W. SHU, *Convergence of Godunov-type schemes for scalar conservation laws under large time steps*, SIAM J. Numer. Anal., 46 (2008), pp. 2211–2237.

[130] J.-M. QIU, C.-W. SHU, L.-L. FENG, AND L.-Z. FANG, *A WENO algorithm for the radiative transfer and ionized sphere at reionization*, New Astronomy, 12 (2006), pp. 1–10.

[131] J.-X. QIU AND C.-W. SHU, *On the construction, comparison, and local characteristic decomposition for high order central WENO schemes*, J. Comput. Phys., 183 (2002), pp. 187–209.

[132] J.-X. QIU AND C.-W. SHU, *Finite difference WENO schemes with Lax–Wendroff-type time discretizations*, SIAM J. Sci. Comput., 24 (2003), pp. 2185–2198.

[133] J.-X. QIU AND C.-W. SHU, *Hermite WENO schemes and their application as limiters for Runge-Kutta discontinuous Galerkin method: One dimensional case*, J. Comput. Phys., 193 (2003), pp. 115–135.

[134] J.-X. QIU AND C.-W. SHU, *Runge–Kutta discontinuous Galerkin method using WENO limiters*, SIAM J. Sci. Comput., 26 (2005), pp. 907–929.

[135] J.-X. QIU AND C.-W. SHU, *A comparison of troubled-cell indicators for Runge–Kutta discontinuous Galerkin methods using weighted essentially nonoscillatory limiters*, SIAM J. Sci. Comput., 27 (2005), pp. 995–1013.

[136] J.-X. QIU AND C.-W. SHU, *Hermite WENO schemes and their application as limiters for Runge–Kutta discontinuous Galerkin method II: Two dimensional case*, Comput. & Fluids, 34 (2005), pp. 642–663.

[137] J.-X. QIU AND C.-W. SHU, *Hermite WENO schemes for Hamilton-Jacobi equations*, J. Comput. Phys., 204 (2005), pp. 82–99.

[138] A. RAULT, G. CHIAVASSA, AND R. DONAT, *Shock-vortex interactions at high Mach numbers*, J. Sci. Comput., 19 (2003), pp. 347–371.

[139] P. ROE, *Approximate Riemann solvers, parameter vectors and difference schemes*, J. Comput. Phys., 27 (1978), pp. 1–31.

[140] T. Schuller, S. Ducruix, D. Durox, and S. Candel, *Modeling tools for the prediction of premixed flame transfer functions*, Proc. Combust. Inst., 29 (2003), pp. 107–113.
[141] T. Schuller, D. Durox, and S. Candel, *A unified model for the prediction of laminar flame transfer functions: Comparisons between conical and V-flame dynamics*, Combust. Flame, 134 (2003), pp. 21–34.
[142] K. Sebastian and C.-W. Shu, *Multi domain WENO finite difference method with interpolation at sub-domain interfaces*, J. Sci. Comput., 19 (2003), pp. 405–438.
[143] S. Serna and A. Marquina, *Power ENO methods: A fifth-order accurate weighted power ENO method*, J. Comput. Phys., 194 (2004), pp. 632–658.
[144] J. Shen, C.-W. Shu, and M. Zhang, *High resolution schemes for a hierarchical size-structured model*, SIAM J. Numer. Anal., 45 (2007), pp. 352–370.
[145] J. Shen, C.-W. Shu, and M. Zhang, *High order WENO schemes for a hierarchical size-structured model*, J. Sci. Comput., 33 (2007), pp. 279–291.
[146] J. Shi, C. Hu, and C.-W. Shu, *A technique of treating negative weights in WENO schemes*, J. Comput. Phys., 175 (2002), pp. 108–127.
[147] J. Shi, Y.-T. Zhang, and C.-W. Shu, *Resolution of high order WENO schemes for complicated flow structures*, J. Comput. Phys., 186 (2003), pp. 690–696.
[148] C.-W. Shu, *Total-variation-diminishing time discretizations*, SIAM J. Sci. Statist. Comput., 9 (1988), pp. 1073–1084.
[149] C.-W. Shu, *Essentially non-oscillatory and weighted essentially non-oscillatory schemes for hyperbolic conservation laws*, in Advanced Numerical Approximation of Nonlinear Hyperbolic Equations, B. Cockburn, C. Johnson, C.-W. Shu, E. Tadmor, and A. Quarteroni, eds., Lecture Notes in Math. 1697, Springer-Verlag, Berlin, 1998, pp. 325–432.
[150] C.-W. Shu, *High order ENO and WENO schemes for computational fluid dynamics*, in High-Order Methods for Computational Physics, T.J. Barth and H. Deconinck, eds., Lecture Notes in Comput. Sci. Engrg. 9, Springer-Verlag, Berlin, 1999, pp. 439–582.
[151] C.-W. Shu, *High order finite difference and finite volume WENO schemes and discontinuous Galerkin methods for CFD*, Internat. J. Comput. Fluid Dynam., 17 (2003), pp. 107–118.
[152] C.-W. Shu, W.-S. Don, D. Gottlieb, O. Schilling, and L. Jameson, *Numerical convergence study of nearly-incompressible, inviscid Taylor-Green vortex flow*, J. Sci. Comput., 24 (2005), pp. 569–595.
[153] C.-W. Shu and S. Osher, *Efficient implementation of essentially non-oscillatory shock capturing schemes*, J. Comput. Phys., 77 (1988), pp. 439–471.
[154] C.-W. Shu and S. Osher, *Efficient implementation of essentially non-oscillatory shock capturing schemes*, II, J. Comput. Phys., 83 (1989), pp. 32–78.
[155] C.-W. Shu, T.A. Zang, G. Erlebacher, D. Whitaker, and S. Osher, *High-order ENO schemes applied to two- and three-dimensional compressible flow*, Appl. Numer. Math., 9 (1992), pp. 45–71.
[156] K. Siddiqi, B.B. Kimia, and C.-W. Shu, *Geometric shock-capturing ENO schemes for subpixel interpolation, computation and curve evolution*, Graphical Models Image Processing (CVGIP:GMIP), 59 (1997), pp. 278–301.
[157] B.A. Steve and D. Levy, *High-order semi-discrete central-upwind schemes for multidimensional Hamilton-Jacobi equations*, J. Comput. Phys., 189 (2003), pp. 63–87.
[158] G. Strang, *Accurate partial difference schemes* II. *Nonlinear problems*, Numer. Math., 6 (1964), pp. 37–46.
[159] D.C. Sun, C.B. Hu, and T.M. Cai, *Computation of supersonic turbulent flowfield with transverse injection*, Appl. Math. Mech., 23 (2002), pp. 107–113.
[160] M. Sussman, P. Smereka, and S. Osher, *A level set approach for computing solutions to incompressible two-phase flow*, J. Comput. Phys., 114 (1994), pp. 146–159.
[161] E. Tadmor, *Convergence of spectral methods for nonlinear conservation laws*, SIAM J. Numer. Anal., 26 (1989), pp. 30–44.
[162] C.K.W. Tam and J.C. Webb, *Dispersion-relation-preserving finite difference schemes for computational acoustics*, J. Comput. Phys., 107 (1993), pp. 262–281.
[163] S. Teramoto, *Large eddy simulation of shock wave boundary layer interaction*, Trans. Japan Soc. Aeronaut. Space Sci., 47 (2005), pp. 268–275.
[164] V.A. Titarev and E.F. Toro, *Finite-volume WENO schemes for three-dimensional conservation laws*, J. Comput. Phys., 201 (2004), pp. 238–260.
[165] V.A. Titarev and E.F. Toro, *ADER schemes for three-dimensional nonlinear hyperbolic systems*, J. Comput. Phys., 204 (2005), pp. 715–736.
[166] E.F. Toro, *Riemann Solvers and Numerical Methods for Fluid Dynamics, a Practical Introduction*, Springer-Verlag, Berlin, 1997.
[167] B. van Leer, *Towards the ultimate conservative difference scheme* V. *A second order sequel to Godunov's method*, J. Comput. Phys., 32 (1979), pp. 101–136.

[168] S. Vukovic and L. Sopta, *ENO and WENO schemes with the exact conservation property for one-dimensional shallow water equations*, J. Comput. Phys., 179 (2002), pp. 593–621.

[169] Z.J. Wang and R.F. Chen, *Optimized weighted essentially nonoscillatory schemes for linear waves with discontinuity*, J. Comput. Phys., 174 (2001), pp. 381–404.

[170] C.C. Wu and T. Chang, *Dynamical evolution of coherent structures in intermittent two-dimensional MHD turbulence*, IEEE Trans. Plasma Sci., 28 (2000), pp. 1938–1943.

[171] Y. Xing and C.-W. Shu, *High order finite difference WENO schemes with the exact conservation property for the shallow water equations*, J. Comput. Phys., 208 (2005), pp. 206–227.

[172] Y. Xing and C.-W. Shu, *High order well-balanced finite difference WENO schemes for a class of hyperbolic systems with source terms*, J. Sci. Comput., 27 (2006), pp. 477–494.

[173] Y. Xing and C.-W. Shu, *High order well-balanced finite volume WENO schemes and discontinuous Galerkin methods for a class of hyperbolic systems with source terms*, J. Comput. Phys., 214 (2006), pp. 567–598.

[174] Y. Xing and C.-W. Shu, *A new approach of high order well-balanced finite volume WENO schemes and discontinuous Galerkin methods for a class of hyperbolic systems with source terms*, Commun. Comput. Phys., 1 (2006), pp. 101–135.

[175] Z. Xu and C.-W. Shu, *Anti-diffusive flux corrections for high order finite difference WENO schemes*, J. Comput. Phys., 205 (2005), pp. 458–485.

[176] Z. Xu and C.-W. Shu, *Anti-diffusive high order WENO schemes for Hamilton-Jacobi equations*, Methods Appl. Anal., 12 (2005), pp. 169–190.

[177] Z. Xu and C.-W. Shu, *Anti-diffusive finite difference WENO methods for shallow water with transport of pollutant*, J. Comput. Math., 24 (2006), pp. 239–251.

[178] R. Wang and R.J. Spiteri, *Linear instability of the fifth-order WENO method*, SIAM J. Numer. Anal., 45 (2007), pp. 1871–1901.

[179] C. Yang and Z.S. Mao, *Numerical simulation of interphase mass transfer with the level set approach*, Chem. Engrg. Sci., 60 (2005), pp. 2643–2660.

[180] H. Yang, *An artificial compression method for ENO schemes: The slope modification method*, J. Comput. Phys., 89 (1990), pp. 125–160.

[181] J.Y. Yang, Y.C. Perng, and R.H. Yen, *Implicit weighted essentially nonoscillatory schemes for the compressible Navier-Stokes equations*, AIAA J., 39 (2001), pp. 2082–2090.

[182] J.Y. Yang, S. Yang, Y. Chen, and C. Hsu, *Implicit weighted ENO schemes for the three-dimensional incompressible Navier-Stokes equations*, J. Comput. Phys., 146 (1998), pp. 464–487.

[183] J.Y. Yang, R.H. Yen, and Y.C. Perng, *Three-dimensional wing flow computations using implicit WENO Euler solvers*, J. Aircraft, 39 (2002), pp. 181–184.

[184] L. Yuan and C.-W. Shu, *Discontinuous Galerkin method based on non-polynomial approximation spaces*, J. Comput. Phys., 218 (2006), pp. 295–323.

[185] N.J. Zabusky, S. Gupta, and Y. Gulak, *Localization and spreading of contact discontinuity layers in simulations of compressible dissipationless flows*, J. Comput. Phys., 188 (2003), pp. 348–364.

[186] M. Zhang, C.-W. Shu, G.C.K. Wong, and S.C. Wong, *A weighted essentially non-oscillatory numerical scheme for a multi-class Lighthill-Whitham-Richards traffic flow model*, J. Comput. Phys., 191 (2003), pp. 639–659.

[187] P. Zhang, S.C. Wong, and C.-W. Shu, *A weighted essentially non-oscillatory numerical scheme for a multi-class traffic flow model on an inhomogeneous highway*, J. Comput. Phys., 212 (2006), pp. 739–756.

[188] Q. Zhang, M. Zhang, G. Jin, D. Liu, and C.-W. Shu, *Modeling, numerical methods and simulation for particle-fluid two phase flow problems*, Comput. Math. Appl., 47 (2004), pp. 1437–1462.

[189] S. Zhang and C.-W. Shu, *A new smoothness indicator for the WENO schemes and its effect on the convergence to steady state solutions*, J. Sci. Comput., 31 (2007), pp. 273–305.

[190] S. Zhang, Y.-T. Zhang, and C.-W. Shu, *Multi-stage interaction of a shock wave and a strong vortex*, Phys. Fluids, 17 (2005), article 116101.

[191] S. Zhang, Y.-T. Zhang, and C.-W. Shu, *Interaction of a shock wave with an oblique vortex pair: Shock dynamics and mechanism of sound generation*, Phys. Fluids, 18 (2006), article 126101.

[192] W. Zhang and A. MacFadyen, *RAM: A relativistic adaptive mesh refinement hydrodynamics code*, Astrophys. J. Suppl. Ser., 164 (2006), pp. 255–279.

[193] Y.-T. Zhang, J. Shi, C.-W. Shu, and Y. Zhou, *Numerical viscosity and resolution of high-order weighted essentially nonoscillatory schemes for compressible flows with high Reynolds numbers*, Phys. Rev. E, 68 (2003), article 046709.

[194] Y.-T. ZHANG AND C.-W. SHU, *High-order WENO schemes for Hamilton–Jacobi equations on triangular meshes*, SIAM J. Sci. Comput., 24 (2003), pp. 1005–1030.

[195] Y.-T. ZHANG AND C.-W. SHU, *Third order WENO scheme on three dimensional tetrahedral meshes*, Commun. Comput. Phys., 5 (2009), pp. 836–848.

[196] Y.-T. ZHANG, C.-W. SHU, AND Y. ZHOU, *Effects of shock waves on Rayleigh-Taylor instability*, Phys. Plasmas, 13 (2006), article 062705.

[197] Y.-T. ZHANG, H.-K. ZHAO, AND J. QIAN, *High order fast sweeping methods for static Hamilton-Jacobi equations*, J. Sci. Comput., 29 (2006), pp. 25–56.

[198] T. ZHOU, Y. LI, AND C.-W. SHU, *Numerical comparison of WENO finite volume and Runge-Kutta discontinuous Galerkin methods*, J. Sci. Comput., 16 (2001), pp. 145–171.